

**PREPARATION OF PELLET CATALYST WITH NON-UNIFORM METAL
DISTRIBUTION**

NG YEE FHAN

**A project report submitted in partial fulfilment of the
requirements for the award of Bachelor of Engineering
(Hons.) Chemical Engineering**

**Lee Kong Chian Faculty of Engineering and Science
Universiti Tunku Abdul Rahman**

April 2015

DECLARATION

I hereby declare that this project report is based on my original work except for citations and quotations which have been duly acknowledged. I also declare that it has not been previously and concurrently submitted for any other degree or award at UTAR or other institutions.

Signature : _____

Name : _____

ID No. : _____

Date : _____

APPROVAL FOR SUBMISSION

I certify that this project report entitled “**PREPARATION OF PELLETT CATALYST WITH NON-UNIFORM METAL DISTRIBUTION**” was prepared by **NG YEE FHAN** has met the required standard for submission in partial fulfilment of the requirements for the award of Bachelor of Engineering (Hons.) Chemical Engineering at Universiti Tunku Abdul Rahman.

Approved by,

Signature : _____

Supervisor : _____

Date : _____

The copyright of this report belongs to the author under the terms of the copyright Act 1987 as qualified by Intellectual Property Policy of Universiti Tunku Abdul Rahman. Due acknowledgement shall always be made of the use of any material contained in, or derived from, this report.

© 2015, Ng Yee Fhan. All rights reserved.

Specially dedicated to
my beloved grandmother, mother and father

ACKNOWLEDGEMENTS

I would like to thank everyone who had contributed to the successful completion of this project. I would like to express my gratitude to my research supervisor, Dr. Yap Yeow Hong for his invaluable advice, guidance and his enormous patience throughout the development of the research.

I would also like to thank my teammates, Tai Xiao Hwa and Neoh Kuang Hong, who worked together with me throughout the research.

In addition, I would like to express my gratitude to my loving parents and friends who had helped and given me encouragement throughout the process of this final year project.

PREPARATION OF PELLET CATALYST WITH NON-UNIFORM METAL DISTRIBUTION

ABSTRACT

Most supported metal catalysts are spherical or cylindrical pellets, with the active catalytic material deposited uniformly within the pellet. The distribution of the catalytic material can have a significant impact on catalyst performance, for example when diffusional resistances are important or when catalyst deactivation is an issue. In this project, platinum on γ -alumina ($\text{Pt}/\gamma\text{-Al}_2\text{O}_3$) catalysts with non-uniform distribution of platinum nanoparticles on the $\gamma\text{-Al}_2\text{O}_3$ support were prepared. Egg-shell catalysts, in which the active catalytic material is preferentially deposited near the outer pellet surface, were prepared by dry impregnation method and charge-enhanced dry impregnation (CEDI) method. Egg-white catalysts, on the other hand have active catalytic material distributed like egg-white were prepared by wet impregnation method. The preparation of metal supported catalysts with non-uniform distribution strongly depends on the concentration of the impregnating solution and drying conditions. However, for strong precursor-support interaction, the drying conditions are not important relative to impregnation. To produce egg-shell catalysts, high concentration of precursor solution should be used. In contrary, low concentration of precursor solution should be used to produce egg-white catalysts. However, drying conditions did not drastically change the metal distribution profile. EDX study has shown that the platinum content in the egg-shell profile produced is more than 5 wt% but for the egg-white profile is only 0.63 wt%. It was also found from TPR study, the optimum reduction temperature is around 212 °C. In addition, FESEM images show that the surface of the catalysts is rough and porous.

TABLE OF CONTENTS

DECLARATION	ii
APPROVAL FOR SUBMISSION	iii
ACKNOWLEDGEMENTS	vi
ABSTRACT	vii
TABLE OF CONTENTS	viii
LIST OF TABLES	xi
LIST OF FIGURES	xii
LIST OF SYMBOLS / ABBREVIATIONS	xv
LIST OF APPENDICES	xvi

CHAPTER

1	INTRODUCTION	1
	1.1 Background	1
	1.2 Problem Statement	1
	1.3 Aim and Objectives	3
	1.4 Scope of Study	3
2	LITERATURE REVIEW	5
	2.1 Catalysts	5
	2.1.1 Types of Catalysts	6
	2.1.2 Heterogeneous Catalysis	7
	2.1.3 Applications of Heterogeneous Catalysis	8
	2.2 Characteristics of Metal Supported Catalyst	10
	2.2.1 Active Catalyst	10

	2.2.2	Catalyst Support	11
2.3		Catalyst Preparation Overview	13
	2.3.1	Impregnation and Drying	14
	2.3.2	Electrostatic Adsorption	17
	2.3.3	Charge-enhanced Impregnation	20
2.4		Diffusion and Adsorption of Metal Precursor	21
	2.4.1	Factors Affecting the Adsorption of Precursor and Final State of Metals	21
2.5		Non-uniform Catalyst Distribution	23
3		METHODOLOGY	26
3.1		Experiments Prior to Catalyst Preparation	26
	3.1.1	Information on Alumina Pellets	26
	3.1.2	Determination of Support PZC (point of zero charge)	27
	3.1.3	Determination of pH for Optimum Metal Uptake	27
3.2		Preparation of Metal Supported Catalysts	28
	3.2.1	Preparation of Egg-shell Catalysts	29
	3.2.2	Preparation of Egg-white Catalysts	29
3.3		Catalyst Characterization	33
	3.3.1	X-Ray Diffraction (XRD)	33
	3.3.2	Scanning Electron Microscope (SEM)	34
	3.3.3	Inductively Coupled Plasma – Optical Emission Spectrometer (ICP-OES)	35
	3.3.4	Field Emission Scanning Electron Microscope (FESEM)	36
	3.3.5	Energy-dispersive X-ray Spectroscopy (EDX)	36
	3.3.6	Temperature-programmed Reduction (TPR)	38
4		RESULTS AND DISCUSSION	39
4.1		γ -Al ₂ O ₃ Pellet Characterization	39
	4.1.1	XRD Results of γ -Al ₂ O ₃ Pellets	39
	4.1.2	SEM Image and EDX Results of Alumina Pellets	40

4.2	Support PZC	41
4.3	Optimum pH for Metal Uptake	42
4.4	Egg-shell Profile	44
4.4.1	Metal Distribution on Alumina	44
4.4.2	FESEM Images and EDX Results	46
4.5	Egg-white Profile	48
4.5.1	Metal Distribution on Alumina	48
4.5.2	FESEM Image and EDX Result	51
4.6	TPR Results	52
5	CONCLUSION AND RECOMMENDATIONS	55
5.1	Conclusion	55
5.2	Recommendations	56
	REFERENCES	57
	APPENDICES	Error! Bookmark not defined.

LIST OF TABLES

TABLE	TITLE	PAGE
2.1	Catalysts in Chemical and Petrochemical Industries (DeJong, 2009)	9
2.2	Catalysts in Pollution Control and Renewable Energy Production (DeJong, 2009)	9
2.3	Types of impregnations (adapted from Regalbuto, 2007)	14
2.4	Distribution of Metal Precursors in Support with Synthesizing Conditions (adapted from Marceau <i>et al</i> , 2009; Lekhal <i>et al</i> , 2007)	25
3.1	Pellet Information provided by Supplier	26
3.2	Settings for different Surface Loadings	27
3.3	Samples prepared and the conditions used	32
3.4	TPR Conditions for Pre-treatment and Analysis	38
4.1	Initial and final pH for different surface loadings	41
4.2	pH and Surface Density of γ -Al ₂ O ₃ Pellets	42

LIST OF FIGURES

FIGURE	TITLE	PAGE
1.1	TEM Image Showing High Dispersion of Pt ₃ Co Nanoparticles (adapted from Kim, 2014)	2
2.1	Activation energy for reaction with and without catalyst (adapted from SchoolWorkHelper)	6
2.2	TEM Image of Ru Nanoparticles on Carbon Catalyst Support (adapted from Su <i>et al.</i> , 2007)	7
2.3	Steps in Heterogeneous Catalysis (adapted from Froment and Bischoff, 1990)	8
2.4	Various Catalyst Supports (adapted from Grecian Magnesite)	12
2.5	Drying Rate and Temperature at Different Stages (adapted from Lekhal <i>et al.</i> , 2007)	17
2.6	Electrostatic Adsorption Mechanism (adapted from Regalbuto, 2007)	17
2.7	Uptake of metal versus pH (adapted from Regalbuto, 2009)	18
2.8	Different surface loadings of alumina support (adapted from Regalbuto, 2007)	19
2.9	pH Shifts with Varying Surface Loadings for Alumina with PZC = 8 (adapted from Regalbuto, 2009)	20
2.10	Non-uniform Catalyst Distribution (adapted from Lekhal <i>et al.</i> , 2007)	23
2.11	Transport phenomena during drying (adapted from Lekhal <i>et al.</i> , 2007)	25

FIGURE	TITLE	PAGE
3.1	Major Steps in the preparation of Egg-shell Catalysts: (a) weighing, (b) impregnation, (c) drying, (d) calcination, and (e) final catalyst	30
3.2	Wet impregnation method where excess solution is used to impregnate the support pellet	31
3.3	XRD-6000 from Shimadzu	33
3.4	Hitachi S-3400N SEM	34
3.5	Emitech Sputter Coater SC7620	35
3.6	PerkinElmer Optima 7000 DV Optical Emission Spectrometer	35
3.7	JEOL JFC-1600 Auto Fine Coater	36
3.8	JEOL FESEM JSM-6701F	37
3.9	TPDRO 1100 Series from Thermo Scientific	38
4.1	XRD Results of γ -Al ₂ O ₃ Pellets	39
4.2	SEM Image of γ -Al ₂ O ₃ Pellet with 5000X magnification	40
4.3	Graph of final pH against initial pH for different Surface Loadings	41
4.4	Graph of Surface Density against Final pH	43
4.5	Metal distribution of sample A (the circled part indicates the flat surface)	44
4.6	Metal distribution of Sample B	45
4.7	FESEM image of Sample A	46
4.8	Platinum Particles Mapping and Element Percentage of Sample A by EDX	47
4.9	FESEM Image of Sample B	48
4.10	Metal Distribution on Alumina; (a) Sample C, (b) Sample D, (c) Sample E, (d) Sample F, and (e) Sample G	49

FIGURE	TITLE	PAGE
4.11	FESEM Image of Sample C	51
4.12	Platinum Particles Mapping and Element Percentage of Sample C using EDX	52
4.13	TPR Curves for Sample A (egg-shell DI), Sample B (egg-shell CEDI), Sample C (egg-white CA 0.2) and Sample E (egg-white CA 1.0)	53

LIST OF SYMBOLS / ABBREVIATIONS

E_a	activation energy
C_f	final metal concentration, mg/L
C_i	initial metal concentration, mg/L
Γ	surface density, nmol/m ²
CPA	chloroplatinic acid
EDX	energy-dispersive X-ray spectroscopy
FESEM	field emission scanning electron microscope
ICP-OES	inductively coupled plasma – optical emission spectrometer
MW	molecular weight, g/mol
OH	hydroxyl group
PZC	point of zero charge
SEM	scanning electron microscope
SL	surface loading, m ² /L
TPR	temperature-programmed reduction
XRD	X-ray diffraction

LIST OF APPENDICES

APPENDIX	TITLE	PAGE
A	Calculation on Surface Loading	61
B	Calculation on Surface Density of γ -Al ₂ O ₃ Pellet after Impregnation	62
C	Calculation on Concentration of Impregnating Solution for Dry Impregnation	63
D	XRD Results of γ -Al ₂ O ₃ pellets	65
E	EDX Results of γ -Al ₂ O ₃ pellets	69
F	ICP-OES Report for Determination of Optimum pH for Maximum Metal Uptake	71
G	EDX Results of Sample A	78
H	EDX Results of Sample C	82
I	TPR Results	85
J	Material Safety Data Sheet (MSDS)	94

CHAPTER 1

INTRODUCTION

1.1 Background

In chemistry, catalysis is the process whereby a chemical reaction is accelerated by a substance termed catalyst. The catalyst itself is not consumed at the end of the reaction and can be reused again. The study of catalysis is crucial for our daily life as it is applied widely in industries and life would cease to exist if biological catalysts (enzymes) are absent.

Catalysts have a wide range of applications in various industries including petrochemical, chemical, refinery, and environmental technology. Current estimates have shown that 85% of chemical processes involve catalysis (DeJong, 2008). The global demand for catalysts has summed up to US\$14.7 billion in year 2011 and is expected to reach US\$19.5 billion in year 2016 with 5.8% annual growth rate (Stephan, 2013). Though catalysts are generally expensive, the products obtained would compensate the cost of catalysts multiple folds.

1.2 Problem Statement

Though catalysts are versatile and receive much attention, relatively little effort was paid to optimizing the performance of catalysts through preparation methods.

One of the common problems for catalysts is that they experience low dispersion (see 2.2.1 c) which might be caused by improper preparation procedures. For metal supported catalysts, low dispersion of metals on the support would lead to low activity and lead to poor catalyst performance. This is because the metals are not fully exposed on the support surface, as they form agglomerates with less surface area. As catalysis only take place on the metal surface, the metals underneath the surface would be wasted as they are unable to carry out reactions when they are not exposed to the reactants. Figure 1.1 shows an example of high dispersion of metals.

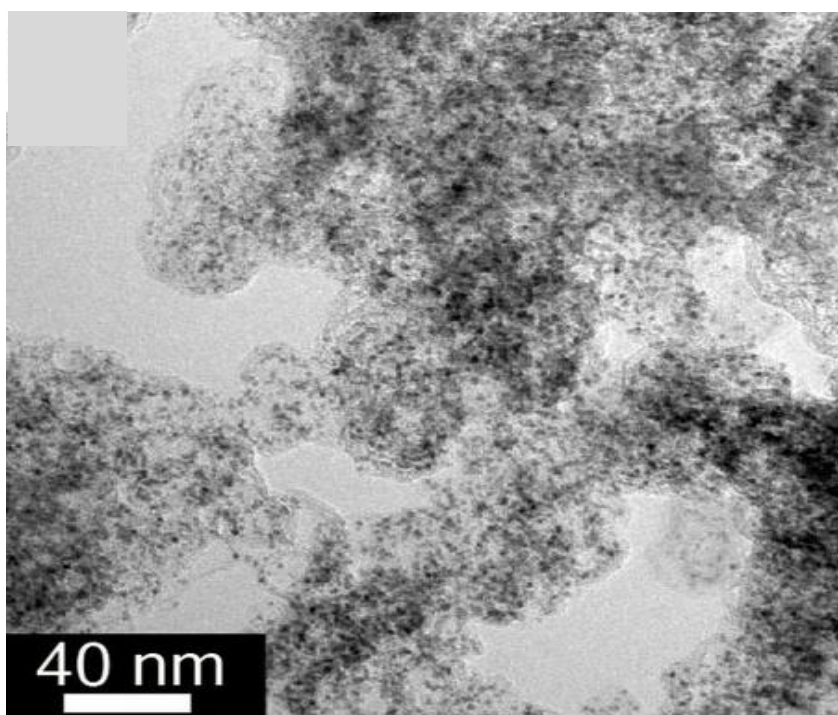


Figure 1.1: TEM Image Showing High Dispersion of Pt₃Co Nanoparticles
(adapted from Kim, 2014)

The distribution of the active catalytic material within the pellet can also have a significant impact on catalyst performance. For example, egg-shell catalysts, in which the active catalytic material is preferentially deposited near the outer pellet surface are mainly used in reactions where diffusional resistances are important (Papageorgiou *et al*, 1996). On the other hand, egg-white and egg-yolk catalysts, in which the active catalytic material distributed towards the inner part of the support

can have the benefit of being less prone to catalyst deactivation (Morbidelli *et al*, 2001).

Many important catalysts are made up of expensive rare noble metals such as platinum, gold, rhodium and etc. Thus, it is important to optimize the performance of the catalysts. Many studies have shown that by altering the method of preparation of the catalysts, a significant improvement in catalytic activity can be achieved and put the metals into efficient use.

1.3 Aim and Objectives

The aim of this project is to produce metal supported catalyst, Pt/Al₂O₃ with non-uniform metal distribution, and to compare the prepared catalysts using several characterization methods. The project aims to achieve the following objectives:

- Investigate the effect of impregnation method (dry impregnation or wet impregnation with coimpregnants) on the metal distribution in within the catalyst pellet
- Investigate the effect of drying conditions on the metal distribution in within the catalyst pellet

1.4 Scope of Study

Two egg-shell profile catalysts were synthesized using both conventional and charge-enhanced dry impregnation method. Other than that, five egg-white profile catalysts were prepared using wet impregnation method with the presence of co-impregnant. The following characterizations were carried out:

- Determination of point of zero charge (PZC) of alumina
- Determination of pH for optimal metal uptake
- Visual inspection of the metal distribution on prepared catalysts

- X-ray diffraction (XRD) of γ -Al₂O₃ pellet
- Scanning electron microscopy (SEM) of γ -Al₂O₃ pellet
- Temperature-programmed reduction (TPR) of prepared catalysts
- Energy-dispersive X-ray spectroscopy (EDX) of prepared catalysts
- Field emission scanning electron microscopy (FESEM) of prepared catalysts

CHAPTER 2

LITERATURE REVIEW

2.1 Catalysts

Catalyst is a substance that is introduced in a chemical process to cause a change in the rate of chemical reaction. Ideally, catalysts remain unspent at the end of reaction though many would age over time. Zeolites, mesoporous materials, alumina and activated carbon are some of the heterogeneous catalysts that are widely applied in the industries.

Here the focus is given to metal supported catalysts. They are made up of a support, which is normally silica, alumina or carbon; and an active catalytic phase – usually metal ions – that is dispersed over the support.

In general catalyst refers to a substance that speeds up reaction. A catalyst does so by introducing an alternative pathway with lower activation energy. Thus, the energy barrier is easier to overcome and the reaction could proceed faster. Figure 2.1 shows the activation energy required for the same reaction without catalyst and with catalyst.

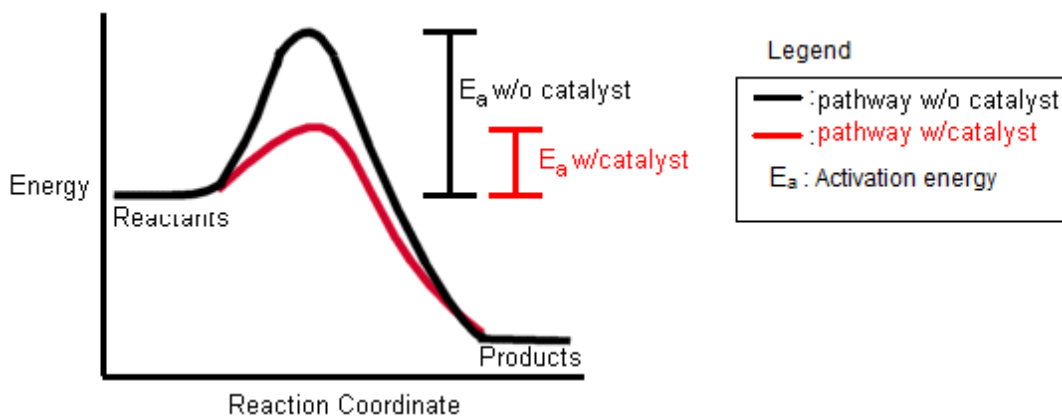


Figure 2.1: Activation energy for reaction with and without catalyst (adapted from SchoolWorkHelper)

2.1.1 Types of Catalysts

There are four types of catalysts:

- **Positive catalyst:** the type of catalyst to increase the rate of reaction.
- **Negative catalyst:** inhibitors; retards the rate of reaction. It is usually used to slow down aging process or decrease the amount of some substances.
- **Auto-catalyst:** catalyst that is a product of a reaction. The reaction starts slowly but after the formation of auto-catalyst, the rate of reaction speeds up.
- **Induced catalyst:** a substance that will induce higher reaction rate in other reactions but not in normal conditions.

Catalysts in the industries could be divided into three classes: heterogeneous catalysts, homogeneous catalysts and enzymes (biocatalysts). Heterogeneous catalysts are catalysts with different phase as the reactants. Typical examples are solid catalysts with liquid or gas phase reactants. Homogeneous catalysts are catalysts with the same phase as the reactants. Enzymes are biological catalysts in the bodies of living things but some are commercialized such as lipase and protease.

The most common type of catalyst used in the industries is solid catalysts. Catalytic processes uses 80% of solid catalysts while homogenous catalysts make up 17% and biocatalysts make up 3% (De Jong, 2009). The advantages of

heterogeneous catalyst include easy separation, efficient recycling and improved handling, which is why they are often favoured in the industry.

The focus of this project is the metal supported catalyst, which falls under the category of heterogeneous catalysts. In general term, metal supported catalysts are catalysts that consist of small metal crystallites (nanoparticles) deposited on a high surface area support. One such example is the Ru/C catalyst for hydrogenation reaction (see Figure 2.2), where ruthenium nanoparticles (3 – 7 nm) are the active catalytic material and anchored the high surface area carbon support. The Ru nanoparticles are the components that are responsible for the hydrogenation reaction.

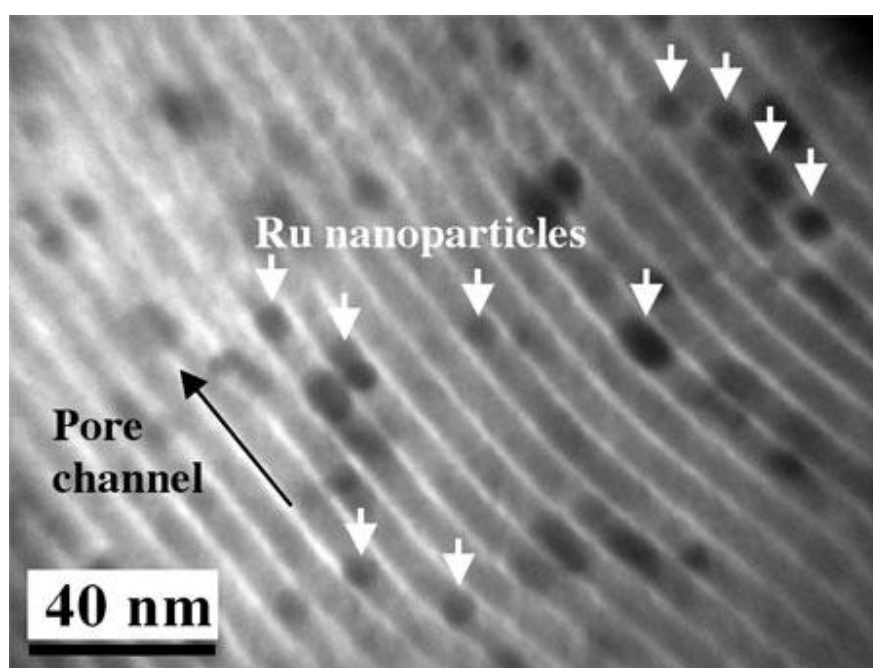


Figure 2.2: TEM Image of Ru Nanoparticles on Carbon Catalyst Support
(adapted from Su *et al*, 2007)

2.1.2 Heterogeneous Catalysis

The process of heterogeneous catalysis can be divided into seven steps (as shown in Figure 2.3):

1. External diffusion of reactants from the bulk fluid to the external surface of the catalyst.

2. Internal diffusion of reactants to the catalyst from the pore mouth through the catalyst pores.
3. Adsorption of reactants onto the active sites of catalysts.
4. Surface reaction at the active sites to convert reactants to products.
5. Desorption of products from active sites.
6. Internal diffusion of the products to the surface through the pores to the pore mouth.
7. External diffusion of the products from the external surface of catalysts to the bulk fluid.

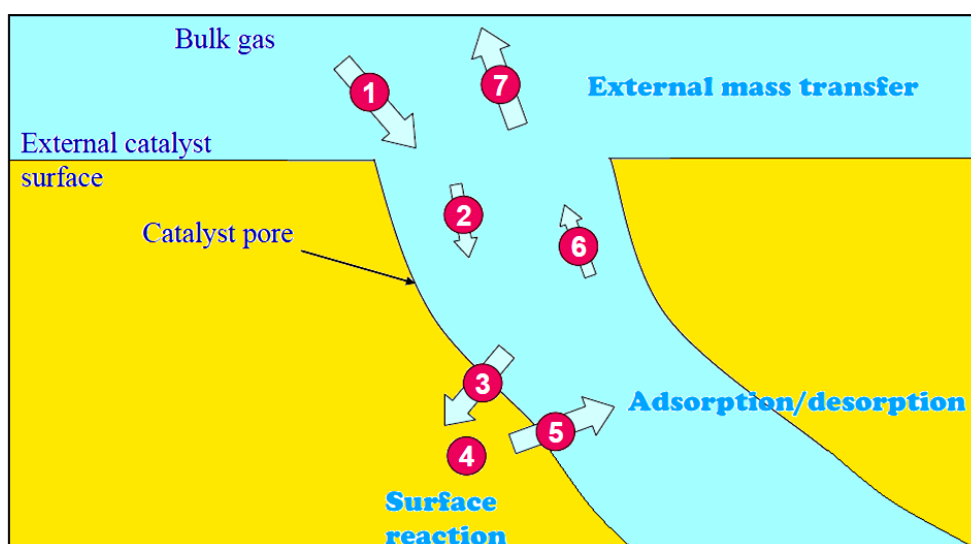


Figure 2.3: Steps in Heterogeneous Catalysis (adapted from Froment and Bischoff, 1990)

2.1.3 Applications of Heterogeneous Catalysis

Heterogeneous catalysts are used extensively in pollution control, chemical synthesis and production and renewable energy production. Perhaps the most widely known heterogeneous catalysis process is the conversion of NO_x and CO in automobiles to carbon dioxide and water vapour.

Table 2.1 and Table 2.2 summarized some catalysts and their applications in the industries. The first table summarizes the catalyst type with their applications in

chemical and petrochemical industries, whereas the second table summarizes their applications in pollution control and renewable energy production.

From Table 2.1 and 2.2, we could see that most of the industrial processes employed metal supported catalysts. Noble metals are used extensively as the active phase in supported catalyst due to their superior activity, selectivity and stability compared to other type of metals.

Table 2.1: Catalysts in Chemical and Petrochemical Industries (DeJong, 2009)

Catalyst	Applications
Ni/SiO ₂	Hydrogenation
K ₂ O/Al ₂ O ₃ /Fe	Ammonia synthesis
CrO _x /SiO ₂	Polymerization
Cu/ZnO/Al ₂ O ₃	Methanol synthesis
Pt/Mordenite	Hydroisomerization of light alkanes
V ₂ O ₅ /SiO ₂	Sulphuric acid synthesis
Pt or Rd wire gauze	Nitric acid synthesis
Zeolite	Catalytic cracking of gas oil

Table 2.2: Catalysts in Pollution Control and Renewable Energy Production (DeJong, 2009)

Catalyst	Applications
Pt	Catalytic converter in automobiles
Pt/C	Hydrogenation in fuel cell
Dolomite	Gasification of biomass
Ni	Decomposition of tars in gas cleanup
Co/SiO ₂	Fischer-Tropsch synthesis

2.2 Characteristics of Metal Supported Catalyst

In this section, the properties that would affect the performance of metal supported catalysts are discussed. To enable better discussion, it is convenient to separate the heterogeneous catalysts to two parts: active catalyst and catalyst support.

2.2.1 Active Catalyst

Active catalysts are the components that are responsible for the reactions. Many of the supported catalysts employ transition metals as the active catalytic material because their outermost d-orbitals are not completely filled with electrons, therefore they could easily donate and accept electrons and result in high activity. The factors that will affect the characteristics and performance of the active catalyst are discussed below:

a) Type of metal

Different metals give different catalytic reactivity. In a research done by Wan Abu Bakar *et al* (2013), alumina supported manganese-nickel oxide based catalysts were used for the conversion of carbon dioxide to methane. The conversion to methane was around 15 to 17.50%. However, when noble metals such as palladium and ruthenium were used, the conversion could go up to 49% at the same reaction temperature. Thus, it could be seen that noble metals have higher activity.

b) Presence of promoter

Promoter is sometimes added in small quantity for better stability or selectivity. A study by Mohammed *et al* (2008) on isomerisation found that the addition of metal promoters such as Sn, Ti and Ni would lead to higher catalytic activity as compared to unpromoted ones. Similarly, in a study done by Farias *et al* (2011), they have found that inclusion of potassium promoter in iron-based catalyst would result in higher activity in Fischer-Tropsch synthesis.

c) Dispersion and size of nanoparticles

Dispersion is the percentage of surface atoms over the amount of actual metal atoms used. Low dispersion causes wastage and poor catalytic performance. Metal catalysts used are mostly noble metals and should be fully utilized. Thus size of metal catalysts should be small so that more surface area are available for surface reaction to take place. Studies conducted (Anderson, 2009; Wang *et al*, 2009; Lin *et al*, 2013) have shown that the smaller the particle size, the higher the reaction rate. However, after an optimum size, further reducing the size would cause declined reaction rate. Lin *et al* (2013) explained that the deviation of metallic nature or different structures might cause this as the size is decreased; whereas Wang *et al* (2009) inferred that small nanoparticles would agglomerate and affects dispersion.

d) Distribution

Distribution is the ‘placement’ of metals on the support, would lead to different effects of catalytic activity, depending on the nature of the reactants or support. Distribution of metals on the support could be uniform or non-uniform. Examples of catalysts with non-uniform distribution of metals are eggshell, egg yolk and egg white profiles. These would be discussed in more detail in Section 2.5.

2.2.2 Catalyst Support

Catalyst supports come in many forms and shapes (see Figure 2.4). They are typically made of refractory materials such as alumina and silica that is able to withstand high reaction temperature. In addition, they usually have high porosity and surface area to disperse the metal nanoparticles. In many instances, the support material may also participate in the catalytic reactions (Bagheri *et al*, 2014).



Figure 2.4: Various Catalyst Supports (adapted from Grecian Magnesite)

a) Type of support

Different catalyst supports are used in different areas as their characteristics differ. In a research by Gao *et al* (2011) regarding catalytic activity of gold clusters using inert hexagonal boron nitride (h-BN) support and active support of TiO₂, it was found that for the regular defect-free surface of h-BN, gold particles interact weakly. In the TiO₂ support, gold particles possess high catalytic activity. Similarly in a research by Dahee *et al* (2014), catalytic activity of platinum nanoparticles differs with supports. They relate the effect with different charge transport between the metal and the support.

b) Specific surface area of porous structure

Catalyst supports are usually made from porous material with high surface area. As specific surface area increases, catalytic activity would be higher due to the presence of more sites for reaction. In a research by Laosiripojana and Assabumrungrat (2006) for methanol decomposition across high and low surface area of CeO₂, it was found that the one with higher surface area achieved higher conversion of methanol to other substances. However sometimes high surface area does not indicate good performance as there might be different metal loadings at the sites.

c) Pore structure and pore size

Pore structure is important as it would influence diffusional limitations in a reaction. Preferably the pore structure should be less tortuous so that particles could

travel faster. In a research by Song *et al* (1991) that investigates hydroprocessing of heavy coal liquids, they infer that larger pore size (macropores) is preferable when comparing support types. However, they recommended catalyst support with bimodal pore size distribution consisting of mesopores and macropores for the hydroprocessing of heavy coal liquids which has shown to have better activity.

d) Mechanical strength

In general, higher mechanical strength of support is preferable as it provides the catalyst resistance towards crushing. Attrition occurs in fluidized-bed reactor, and if the support has low mechanical strength, it will form fines and carried away by the product flow. Mechanical strength is influenced by shape and porosity of support. Generally, higher porosity would lead to lower mechanical strength.

e) Shape and size

Liu and Roy (2004) have performed a research by altering the channel shape and channel size of monolith catalyst to investigate its effect on three-phase catalytic reaction. Three reactions were carried out in 2 mm and 1 mm size channels for circular and square shape. It was found that the circular shaped support has higher activity compared to that of square shaped support as there is stagnant liquid in the square channel (Liu and Roy, 2004). The reduction of channel size causes the contacting efficiency of gas/liquid/solid to increase due to the surface tension and reduced mass transfer distance. However, further improvement could not be attained if the support surface is already effectively utilized using a particular size; instead the enhancement of degree of activity by channel shape drops with the decrement of channel size (Liu and Roy, 2004).

2.3 Catalyst Preparation Overview

According to DeJong (2009), there are many techniques available for the preparation of catalyst: shaping, impregnation, deposition precipitation, hydrothermal synthesis and chemical vapour deposition (CVD). In this literature review, focus is given to impregnation technique. Impregnation is the contact between a solid and a liquid

phase, and the liquid phase is adsorbed by the solid phase (Marceau *et al*, 2009). Details are provided in Section 2.3.1.

2.3.1 Impregnation and Drying

Impregnation is probably the most widespread technique in preparing supported metal catalysts as it is relatively cheap and simple. In this technique, a catalyst support, normally oxides (alumina, silica) or carbon is contacted with metal complexes dissolved in liquid solutions (metal precursors). During impregnation, there are several processes that take place (IUPAC, 1995):

- Selective adsorption by Coulomb forces, Van der Waals forces and hydrogen bonds;
- Ion exchange of the charged surface and the impregnating solution;
- Polymerisation or depolymerisation of the species on the surface;
- Partial disintegration of the solid surface.

The types of impregnations are summarized in Table 2.3 (Regalbuto, 2007; IUPAC, 1995).

Table 2.3: Types of impregnations (adapted from Regalbuto, 2007)

Type of impregnations	Characteristics
Dry impregnation	Just enough amount of impregnating solution is used to fill up the pore volume of the catalyst support.
Wet impregnation	Excess amount of impregnating solution is used to fill up the volume of the catalyst support.
Co-impregnation	Two or more species are introduced to the catalyst support simultaneously in impregnation process.
Strong electrostatic adsorption	Using excess solution; pH used is altered for optimum precursor-support interaction.

In wet impregnation, the impregnating solution used is in excess amount and the metal complexes would diffuse to adsorb on the surface of the catalyst support. This method is generally avoided when the precursor does not strongly interact with the support as it would cause the metal complexes to be wasted. Generally, the distribution of the solute depends on the diffusion of solute into the catalyst pores and the adsorption of the solute on the catalyst support. Adsorption depends on the adsorption equilibrium constant and the adsorption capacity of the surface (Marceau *et al*, 2009).

In dry impregnation, the volume of impregnating solution of the metal precursor is just enough to fill up the pore volume of catalyst support. Capillary action draws the solution inwards of the catalyst pores which is significantly faster than the diffusion process in wet impregnation. The pore volume initially filled with air has to be vacuumed to ensure the liquid phase is able to penetrate during impregnation. This is because liquid penetration halts when capillary pressure equates the pressure of entrapped air. However, capillary pressure is much higher than the pressure of entrapped air when pellet radius is small, which renders the elimination of air unnecessary. Sometimes bubbles will form when the flow is not sufficiently reduced. The formation of bubbles might cause the catalyst grain to burst as it is not designed to oppose such force. This could be solved by impregnating under the catalysts vacuum conditions (Cao *et al*, 2014).

During impregnation, parameters such as viscosity and concentration could alter the final distribution of metals. Details could be found in Section 2.5.

Drying is a thermally activated step to eliminate the solvent of impregnating solution after the impregnation process. It is done by heating the impregnated catalyst in an oven at the boiling temperature of the solvent. Alternatively, it could also be subjected to lower temperature in static conditions or with a flow of gas. When solvent vaporizes, the metal precursor concentration increases, they crystallize and are adsorbed to the support surface. Thus, the metal precursor is reduced to its active elemental state (Lekhal *et al*, 2007).

Drying could be divided into three stages: the preheating period, the constant rate period and the falling rate period. During preheating, the catalyst support is heated up and the rate of drying increases with temperature. At constant rate period, rate of drying is constant, and thus vapour is constantly removed from the surface of the support (Lekhal *et al.*, 2007). Capillary flow makes sure the liquid is transported to the surface (Lekhal *et al.*, 2007). During falling rate period, the vapour removal is faster than the liquid transport to the surface, and thus drying rate decreases. The drying front recedes from the external surface of the catalyst and the surface dries. Figure 2.5 illustrates the drying rate and the temperature of catalyst support at different stages of drying.

During drying, transport phenomena such as convective flow of solvent towards the pellet surface and the back-diffusion of metal (solutes) to the center of the pellet take place. According to Lee and Aris (1985), there will also be redistribution of metals. Thus the final distribution of metals depends on the balance between transport and adsorption of metal precursor.

One of the important factors to be considered during drying is temperature. Despite the fact that high temperature should be applied for higher evaporation rate, some hydrated salts melt at moderated temperature, which will cause agglomeration of metal complexes (Marceau *et al.*, 2009). In addition, high temperature may also cause evaporation of non-solvent molecules, for instance, competitors that are volatile.

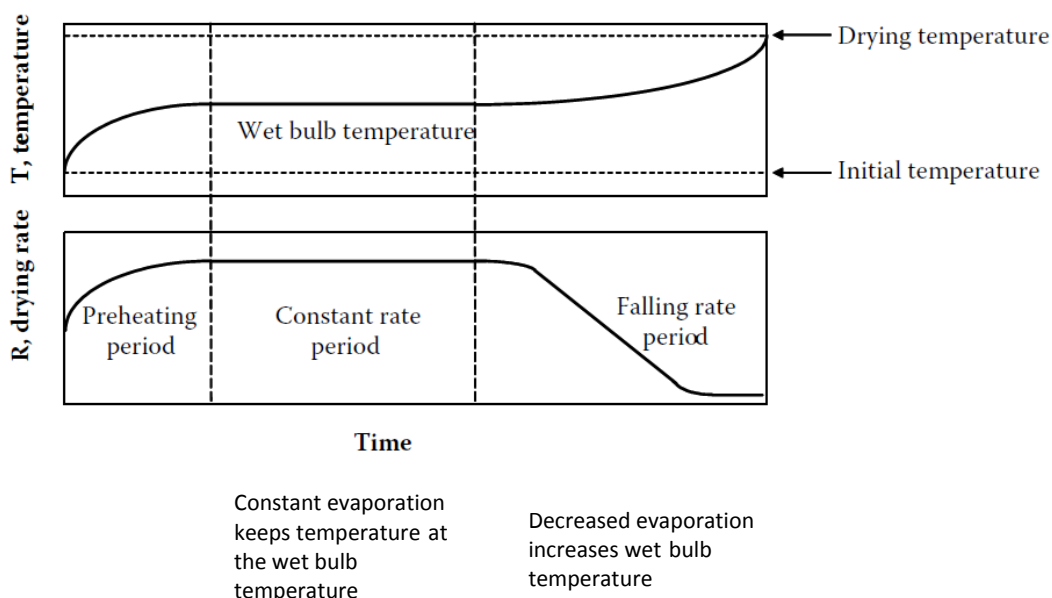


Figure 2.5: Drying Rate and Temperature at Different Stages (adapted from Lekhal *et al*, 2007)

2.3.2 Electrostatic Adsorption

During impregnation the surface of catalyst support is contacted with the impregnating solution, the extent in which the metal ions are retained by the support is affected by physical (electrostatic) and chemical interaction (Regalbuto, 2007). One way to create strong interactions is via electrostatic adsorption mechanism.

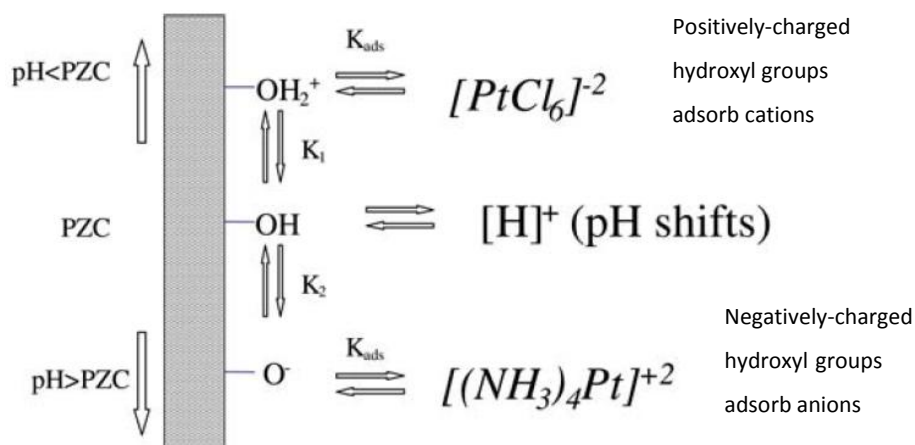


Figure 2.6: Electrostatic Adsorption Mechanism (adapted from Regalbuto, 2007)

Generally, for most oxide supports, the oxides are terminated by hydroxyl groups. The pH of catalyst support when the hydroxyl groups are neutral is called the point of zero charge (PZC). When the pH of the solution is lower than the PZC, protons are present in excessive amount in the solution, so the hydroxyl groups become positively charged and adsorb anions. Above the PZC, there is a lack of protons in the solution, therefore the hydroxyl groups release protons and subsequently become negatively charged and adsorb cations. The mechanism is illustrated in Figure 2.6.

There is an optimum pH in which the metal complexes are adsorbed the most. For example, platinum uptake for anionic platinum hexachloride, $[\text{PtCl}_6]^{-2}$ adsorbing on alumina support increases with decreasing pH but the uptake decreases for further decrement in pH. Regalbuto (2007) has argued that at low pH extremes, high ionic strength inhibits adsorption, resulting in low uptake of platinum as shown in Figure 2.7.

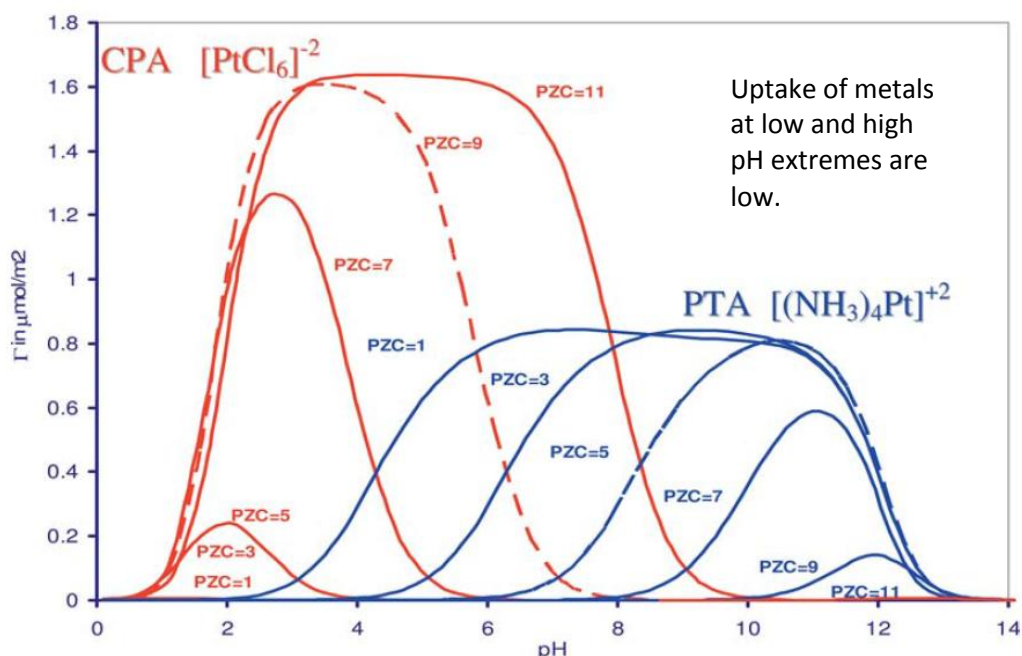


Figure 2.7: Uptake of metal versus pH (adapted from Regalbuto, 2009)

Typically, the pH of the impregnating solution is uncontrolled during catalyst preparation. The final pH of the impregnating solution varies and would end up near

the PZC of the support, where there will be no interaction between metal precursor and support (Regalbuto, 2009). This could be attributed to the pH buffering effect of oxides where the support surface is uncharged due to the high amount of OH groups of the surface compared to that in the impregnating solution. This explains why mild solutions (pH close to PZC) could not significantly charge the surface, where there is little proton transfer and causes the final solution pH to end up near the support PZC (Regalbuto, 2009).

A key parameter to be considered is surface loading, which is defined as the oxide surface area per volume of the solution (Regalbuto, 2007) as illustrated in Figure 2.8. High surface loading can be achieved by dry impregnation because the amount of impregnating solution is just enough to fill the pore volume of the support. High surface loadings result in a final pH near the support PZC due to buffering effect (in Figure 2.9). When the buffering effect is overcome, there would be chance for strong electrostatic adsorption of metal complexes (Regalbuto, 2007).

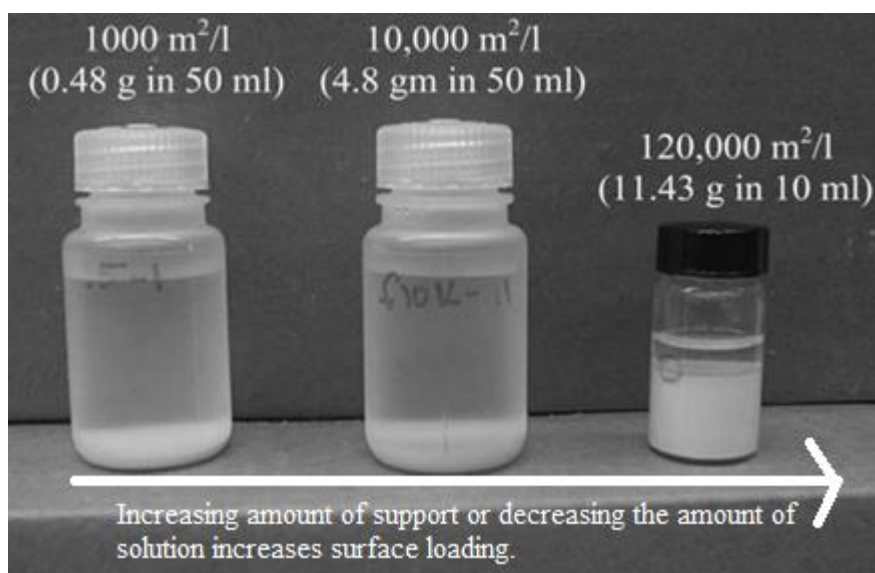


Figure 2.8: Different surface loadings of alumina support (adapted from Regalbuto, 2007)

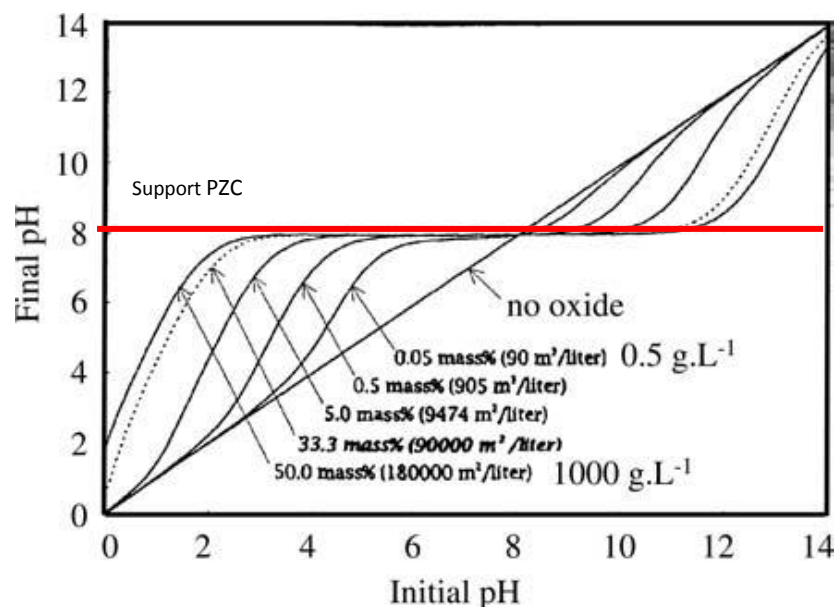


Figure 2.9: pH Shifts with Varying Surface Loadings for Alumina with PZC = 8
(adapted from Regalbuto, 2009)

2.3.3 Charge-enhanced Impregnation

The traditional impregnation method often does not lead to strong precursor-support interaction, which causes undesirable distribution of the metal phase and sintering (Zhu *et al*, 2013). For instance, metal complexes might form agglomerates which would decrease specific surface area and affect the performance of the catalyst. In Section 2.3.2, it was introduced that strong electrostatic adsorption can create strong precursor-support interaction. This is done by using an optimum pH to maximize the adsorption of metal precursors to the support surface.

The convenience of impregnation method and the advantage of strong precursor-support interaction offered by strong electrostatic adsorption can be combined to form charge-enhanced impregnation method (Zhu *et al*, 2013). Charge-enhanced impregnation has been demonstrated to synthesize noble and base metal nanoparticles over various oxides and carbon supports with loadings up to 30 wt%, with wet impregnation using thin slurries and with dry impregnation using thick slurries.

For strong electrostatic adsorption to occur during dry impregnation, the initial pH of the impregnating solution should be adjusted so that the surface could be sufficiently charged. Thus, metals could be adsorbed on the support surface strongly. This will improve the dispersion of metals in pellet catalysts, and thus ensuring the entire deposition of metals. However, buffer effect can be significant for catalyst support that has high surface area. Therefore, to protonate or deprotonate all the surface OH groups, either extremely basic or extremely acidic solutions is required to overcome the buffer effect and causes the final pH to end up near the support PZC.

2.4 Diffusion and Adsorption of Metal Precursor

As described in Section 2.3.1, impregnation of pellet catalyst by an impregnating solution is governed by adsorption and diffusion. The diffusion of the solution in the pores of the support takes place after the liquid front arrives at the centre of the pellet through capillary force. On the other hand, adsorption is the deposition of metal precursors onto the sites of the support.

As the focus of this project is on the non-uniform distribution of metal in a pellet support, it is essential to investigate the factors that determine the adsorption and distribution of metal catalysts and they are discussed in the following subchapters.

2.4.1 Factors Affecting the Adsorption of Precursor and Final State of Metals

a) Solution pH

At certain pH of the solution, the support dissolves and releases ions. According to Santacesaria *et al* (1997), the adsorption of hexachloroplatinate acid on alumina support has dissolved the surface and released aluminium ions. Experiments performed by Heise and Schwarz (1985), Blachou and Philippopoulos (1993), and

Shah and Regalbuto (1994) have also shown that the adsorption of platinum from hexachloroplatinate decreases with decreasing pH (in the range of 0-1) although the uptake initially increases. There were three explanations:

- Heise and Schwarz (1985) attributed this with the dissolution of alumina;
- Blachou and Philippopoulos (1993) has explained that this due to the pH dependency for formation of platinum complexes with different affinity for the alumina surface;
- Shah and Regalbuto (1994) explained that this is due to the increased ionic strength of the solution in low pH and thus equilibrium adsorption constant is decreased.

b) Surface heterogeneity

As described by the electrostatic adsorption model in Figure 2.6, when pH is less than the PZC of support, alumina surface will adsorb cations. However, there are cases where the adsorption of cations on alumina could also take place at a pH more than the PZC (Huang *et al.*, 1986; Komiyama *et al.*, 1980). Surface heterogeneity could be used to explain this, which is the existence of different types of sites that would adsorb different ions (Hiemstra *et al.*, 1989; Abello *et al.*, 1995). Wang and Hall (1982) argued that the presence of different crystal planes with different local isoelectric point was the reason for surface heterogeneity. Different ions from the impregnating solution at different pH could be used to interact with the support surface.

c) Ionic strength

Ionic strength of the impregnating solution affects the electric double-layer thickness and activity coefficient of metal ions (Heise and Schwarz, 1986). As ionic strength increases, the uptake of metal precursors decreases, due to the shielding effect of the electric field of the surface. This results in decreased attraction between metal ions and support surface, which decreases the adsorption of metal ions on support surface.

d) Coimpregnants

The presence of coimpregnants in the impregnating solution would compete with the metal precursor for adsorption onto the active sites of the support. Heise and

Schwarz (1990) has shown that different amount of platinate ion is adsorbed with varying concentration of coimpregnants. When there is little coimpregnants in the solution, there is no competition due to large amount of spaces available for adsorption.

2.5 Non-uniform Catalyst Distribution

The dispersion and distribution of metal complexes on pellet catalysts is primarily affected by impregnation, drying and adsorption. The factors that affect the adsorption of metal complexes on the support were discussed in Section 2.4.1, which will not be discussed further in this subchapter. So, the focus in this subchapter is given to the effect of impregnation and drying on the metal distribution in a pellet support.

The common non-uniform catalyst distributions in a spherical shape pellet are egg-shell, egg-white or egg-yolk profile, as shown in Figure 2.10.

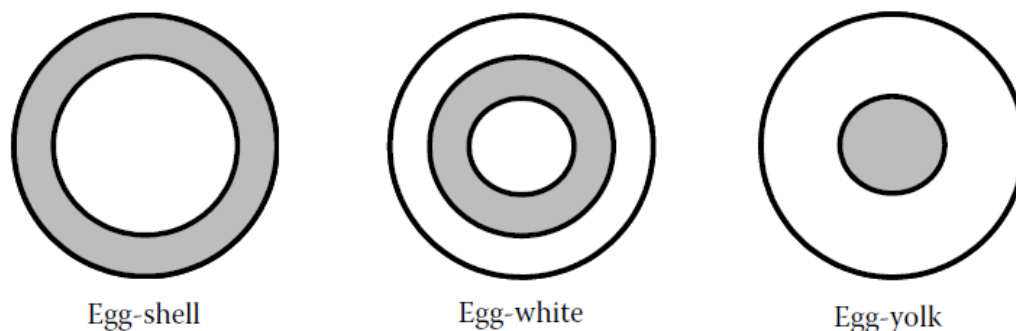


Figure 2.10: Non-uniform Catalyst Distribution (adapted from Lekhal *et al.*, 2007)

During impregnation, concentration of metal complexes and solution viscosity affect the metal complex distribution. Viscosity increases with concentration of metal complexes in the solution (Marceau *et al.*, 2009). High concentration of metal complexes favour the diffusion of solute to the center of the

pellet, but at the same time high viscosity of solution also slows down the diffusion and capillary action. It is predicted that egg-shell profiles are formed from low concentrations of solution with strong adsorption of metal complexes and short impregnation times (Marceau *et al.*, 2009).

To produce egg-white or egg-yolk profiles, competing adsorbates (competitors) could be added (Hepburn *et al.*, 1989; Wang *et al.*, 1984; Heise and Schwarz, 1990). Competitors would compete with the metal ions for adsorption sites on the support surface. The competitors will adsorb on active sites first and thus driving the metal ions to the subsurface layers.

Apart from impregnation, drying also affects the metal complexes distribution in the support. In the porous network, solvent transports metal complexes to the external surface or towards the center (back-diffusion). As discussed in Section 2.3.1, drying can be divided into constant rate and falling rate period, convective flow dominates at constant rate period. At the end of it, the metal complexes concentration is at maximum at the external surface of the pellet (Lekhal *et al.*, 2007). At falling rate period, convective flow decreases or ceases and diffusion dominates. Back-diffusion becomes dominant and transports the metal complexes towards the center of the pellet. Thus, the concentration of metals at the external surface decreases. Figure 2.11 shows the transport phenomena during drying.

Heating rate and drying temperature could affect the transport of solvents. Low heating rate would cause constant rate period to dominate. When there is strong precursor-support interaction, the effect of drying does not affect the metal profile significantly.

Table 2.4 summarizes the conditions to prepare different catalyst profiles.

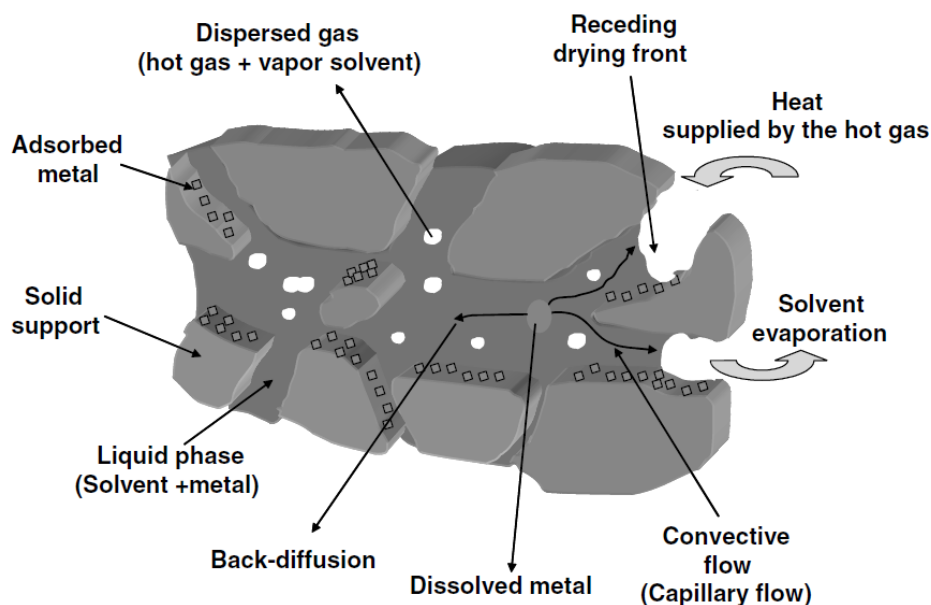


Figure 2.11: Transport phenomena during drying (adapted from Lekhal *et al.*, 2007)

Table 2.4: Distribution of Metal Precursors in Support with Synthesizing Conditions (adapted from Marceau *et al.*, 2009; Lekhal *et al.*, 2007)

Distribution	Conditions
Egg-shell	<ul style="list-style-type: none"> • Impregnation with viscous solution. • Indication of strong precursor-support interaction, with minimal competitor interaction. • Intermediate drying regime with dominant convective flow, in the case of low viscosity and concentration of solution.
Egg-yolk	<ul style="list-style-type: none"> • Impregnation with low viscosity solution. • Stronger interaction between competitors and support surface than the precursor-support. • Fast drying with pronounced back-diffusion.
Uniform	<ul style="list-style-type: none"> • Drying a concentrated, viscous solution. • Equal interaction between precursors and competitors. • Drying under mild conditions for weakly adsorbed metal complexes.

CHAPTER 3

METHODOLOGY

3.1 Experiments Prior to Catalyst Preparation

Prior to catalyst impregnation, the pellet information, support PZC and the optimum pH for metal uptake were determined.

3.1.1 Information on Alumina Pellets

The catalyst support used is 3 mm γ -alumina spherical pellet obtained from Zibo Wufeng Aluminium Magnesium Technology Co. Ltd. The information of alumina pellets was obtained from the supplier and was tabulated in Table 3.1.

Table 3.1: Pellet Information provided by Supplier

Parameter	Specifications
Al ₂ O ₃ content	≥ 92%
SiO ₂ content	≤ 0.1%
Fe ₂ O ₃ content	≤ 0.04%
Na ₂ O content	≤ 0.1%
Bulk density	0.65 g/ml
Surface area	≥ 200 m ² /g
Pore volume	≥ 0.42 ml/g
Crush strength	90 N

3.1.2 Determination of Support PZC (point of zero charge)

The procedure to determine the PZC of γ -alumina spherical pellet is shown below:

1. 200 ml of deionised water was measured (which corresponds to surface loading of 50 m²/L).
2. Hydrochloric acid was added until the pH of the solution reaches around 2.
3. The initial pH of the solution was measured using a pH meter.
4. 0.05 g of crushed alumina pellets was added into the solution.
5. The solution with alumina pellets was stirred using magnetic stirrer for 8 minutes.
6. The solution with alumina pellets was then left for 10 minutes.
7. The final pH of the solution was measured using a pH meter.
8. The steps were repeated for different pH (for high pH, sodium hydroxide was used instead of hydrochloric acid).
9. The steps were repeated for different surface loadings as in Table 3.2 by calculating using the formula below (sample calculation included in Appendix A):

$$\text{Surface Loading} \left(\frac{\text{m}^2}{\text{L}} \right) = \frac{\text{BET surface area} \left(\frac{\text{m}^2}{\text{g}} \right) \times \text{Mass of pellet}}{\text{Volume of solution}} \quad (3.1)$$

Table 3.2: Settings for different Surface Loadings

Surface loading (m²/L)	50	500	1000
Volume of deionized water (mL)	200	20	10
Mass of alumina pellets (g)	0.05	0.05	0.05

3.1.3 Determination of pH for Optimum Metal Uptake

The procedure to determine the optimum pH for optimum metal uptake is shown below:

1. 50 mL of 600 ppb of CPA in deionized water was prepared.
2. Hydrochloric acid was added until the pH reaches around 2.

3. The initial pH was measured using a pH meter.
4. The CPA solution prepared was separated into two centrifuge tubes (centrifuge tube A and B) with 15 mL of solution each. Centrifuge tube B was used to test initial metal concentration using ICP.
5. 0.045 g of alumina pellet was crushed (corresponds to $SL = 600 \text{ m}^2/\text{L}$)
6. The crushed alumina pellet was added to centrifuge tube A.
7. Centrifuge tube A was shaken for 1 hour.
8. The alumina pellets were filtered and the supernatant of centrifuge tube A was transferred to centrifuge tubes C and D.
9. Centrifuge tube C (with 8 mL of solution) was sent for ICP analysis to determine the final metal concentration after impregnation.
10. Centrifuge tube D (with 5 mL of solution) was used to measure the final pH.
11. The steps were repeated to produce a range of pH (for high pH, sodium hydroxide was used instead of hydrochloric acid).
12. Surface density was calculated using the equation below (sample calculation included in Appendix B):

$$\text{Surface density, } \Gamma \left(\frac{\text{nmol}}{\text{m}^2} \right) = \frac{(C_i - C_f) \left(\frac{\text{mg}}{\text{L}} \right) \times 10^9 \left(\frac{\text{nmol}}{\text{mol}} \right)}{SL \left(\frac{\text{m}^2}{\text{L}} \right) \times MW \text{ of metal} \left(\frac{\text{g}}{\text{mol}} \right) \times 1000 \left(\frac{\text{mg}}{\text{g}} \right)} \quad (3.2)$$

Where

- C_i = Metal initial concentration
 C_f = Metal final concentration
 SL = Surface loading
 $MW \text{ of metal}$ = Molecular weight of metal

3.2 Preparation of Metal Supported Catalysts

Chloroplatinic acid hexahydrate (CPA) obtained from Yurui (Shanghai) Chemical Co. Ltd. was used as the metal precursor in this project. The aim of this project is to prepare metal supported catalyst with non-uniform distribution. Two types of distribution have been prepared:

- i) Egg-shell catalyst
- ii) Egg-white catalyst

For the egg-white catalyst, citric acid-1-hydrate obtained from HmbG Chemicals is used as a coimpregnant. The steps the preparation of egg-shell catalysts and egg-white catalysts are described in the following subchapters.

3.2.1 Preparation of Egg-shell Catalysts

1. 1 g of alumina pellets was measured using a weight balance.
2. CPA with a concentration of 0.1226 g/mL was prepared (calculation on the concentration provided in Appendix C).
3. 450 μ L of solution was extracted using micropipette and the pellets were impregnated.
4. The impregnated pellets were then left for 15 minutes before drying at 120 $^{\circ}$ C for 18 hours.
5. The pellets were calcined in air at 500 $^{\circ}$ C for 5 hours.
6. Characterization of catalysts was carried out.
7. Steps 1 and 2 were repeated. Hydrochloric acid was added to the chloroplatinic acid hexahydrate solution.
8. Steps 3 to 6 were repeated.

3.2.2 Preparation of Egg-white Catalysts

1. 1 g of alumina pellets was measured using a weight balance.
2. 2 mL of CPA with a concentration of 0.04 M was prepared.
3. 2 mL of citric acid-1-hydrate with a concentration of 0.2 M was prepared.
4. The two solutions above were mixed together to form a new solution.
5. The alumina pellets were inserted to the new solution.
6. The pellets and solution were left for 15 minutes.

7. The pellets were taken out and washed using deionized water.
8. The pellets were dried at 180 °C for 4 hours to remove the solvent from the pores.
9. The pellets were then calcined in air at 500 °C for 5 hours.
10. Characterization of catalysts was carried out.
11. Steps 1 to 10 were repeated for citric acid concentrations of 0.5 M, 1.0 M and 1.5 M with different impregnation time and drying conditions.

Figure 3.1 shows the procedure of preparing egg-shell catalysts with images. For egg-white catalysts, the impregnation method (Step (b)) was changed to wet impregnation as shown in Figure 3.2.

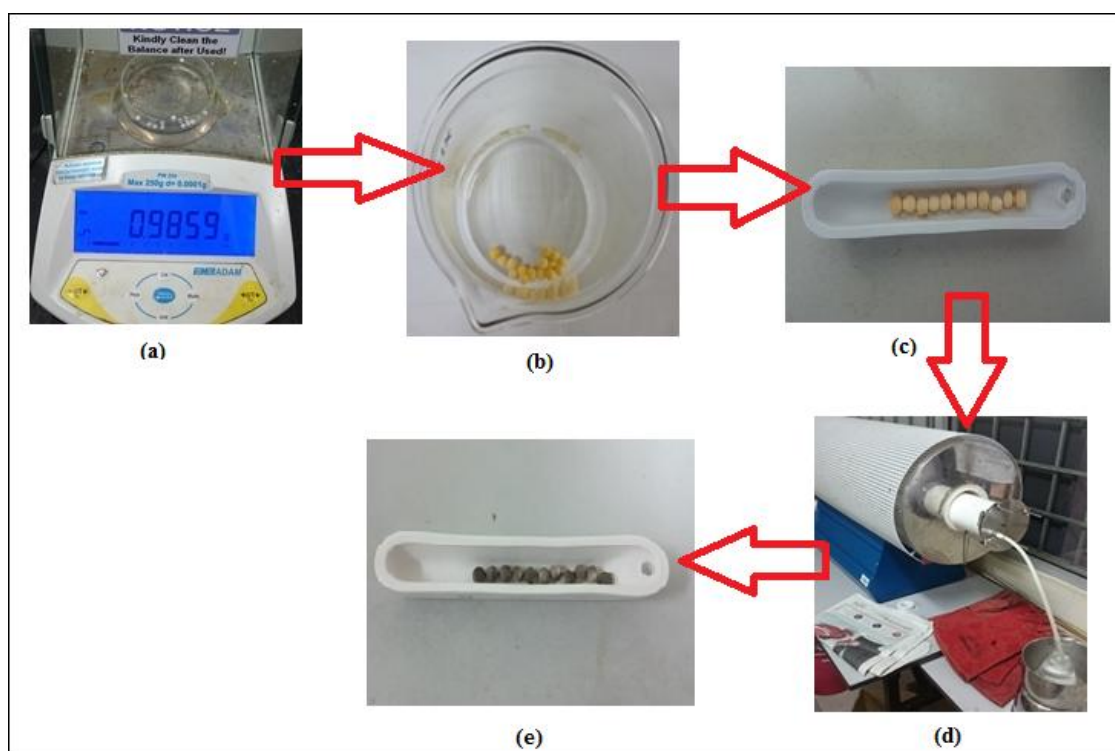


Figure 3.1: Major Steps in the preparation of Egg-shell Catalysts: (a) weighing, (b) impregnation, (c) drying, (d) calcination, and (e) final catalyst



Figure 3.2: Wet impregnation method where excess solution is used to impregnate the support pellet

Following the preparation of catalysts by impregnation, the pellet catalysts were grinded using diamond file, while placing the catalyst in a well of a metal plate. This is to observe the cross-sectional view of the catalyst. The distribution of metal was investigated with the help of microscope.

Table 3.3 in the next page summarizes the samples generated and the preparation conditions.

Table 3.3: Samples prepared and the conditions used

Profile	Egg-shell		Egg-white				
Sample Designation	A	B	C	D	E	F	G
Preparation method	Dry impregnation	Charge-enhanced dry impregnation	Wet impregnation	Wet impregnation	Wet impregnation	Wet impregnation	Wet impregnation
Concentration of CPA (M)	0.24	0.24	0.04	0.04	0.04	0.04	0.04
Mass of CPA (g)	0.0544	0.0544	0.0414	0.0414	0.0414	0.0414	0.0414
Presence of co-impregnant	No	No	Yes, citric acid				
Concentration of citric acid (M)	-	-	0.20	0.50	1.00	1.00	1.50
Mass of citric acid (g)	-	-	0.084	0.210	0.420	0.420	0.630
Volume of impregnating solution (mL)	0.45	0.45	4	4	4	4	4
Impregnation time	-	-	15 minutes	1 hour	30 minutes	1 hour	1 hour
Drying conditions	120 °C for 18 hours	120 °C for 18 hours	180 °C for 4 hours	120 °C for 4 hours			

3.3 Catalyst Characterization

The surface structure and the chemical composition of a catalyst are important factors that determine its performance. In this section the methods to characterize a catalyst are described. Four types of equipments were used for characterization purposes: XRD, SEM, ICP-OES, TPR, FESEM and EDX.

3.3.1 X-Ray Diffraction (XRD)

XRD-6000 by Shimadzu is used to study the phase of the alumina pellets. The alumina pellets were crushed to powder form and placed on the sample holder. The diffractometer was operated at 40 kV and 30 mA with Cu K_{α} of $\lambda = 1.54\text{\AA}$. The deflection angle, 2θ , was then set to scan from 10° to 80° with a scanning rate of $2^{\circ}/\text{min}$. Figure 3.3 shows the XRD equipment.



Figure 3.3: XRD-6000 from Shimadzu

3.3.2 Scanning Electron Microscope (SEM)

Hitachi S-3400N SEM (see Figure 3.4) is used to view the structure of alumina pellets. An alumina pellet was placed on the sample holder with a carbon tape. The sample was coated with palladium and gold using Emitech Sputter Coater SC7620 (Figure 3.5) to make the sample conductive. The focal length used was 6.2 mm and the applied voltage is 15 kV. The magnifications of alumina pellets were set to 5000X.



Figure 3.4: Hitachi S-3400N SEM



Figure 3.5: Emitech Sputter Coater SC7620

3.3.3 Inductively Coupled Plasma – Optical Emission Spectrometer (ICP-OES)

ICP-OES is used to determine the metal uptake of alumina for different pH using PerkinElmer Optima 7000 DV Optical Emission Spectrometer (see Figure 3.6). The calibration of platinum was done using PerkinElmer Pure Plus Multi-Element Calibration Standard 4 with concentration of 10 mg/L. The standard solutions prepared range from 20 ppb to 300 ppb.



Figure 3.6: PerkinElmer Optima 7000 DV Optical Emission Spectrometer

3.3.4 Field Emission Scanning Electron Microscope (FESEM)

Like SEM, FESEM was used to view the morphology of the catalyst sample. The main difference between them is that FESEM allows higher magnification. The model of FESEM used for sample analysis is JSM-6701 from JEOL (refer Figure 3.8). The principle of using FESEM is almost the same as SEM: Alumina pellets were crushed and placed on the sample holder with a carbon tape. The samples were coated with platinum using JEOL JFC-1600 Auto Fine Coater (refer Figure 3.7) to make the sample conductive. The samples were degassed in a chamber before turning on the electron gun. The magnification is set to 30 000X and 70 000X. The working distance used is 6.1 mm and the voltage applied is 2 kV.

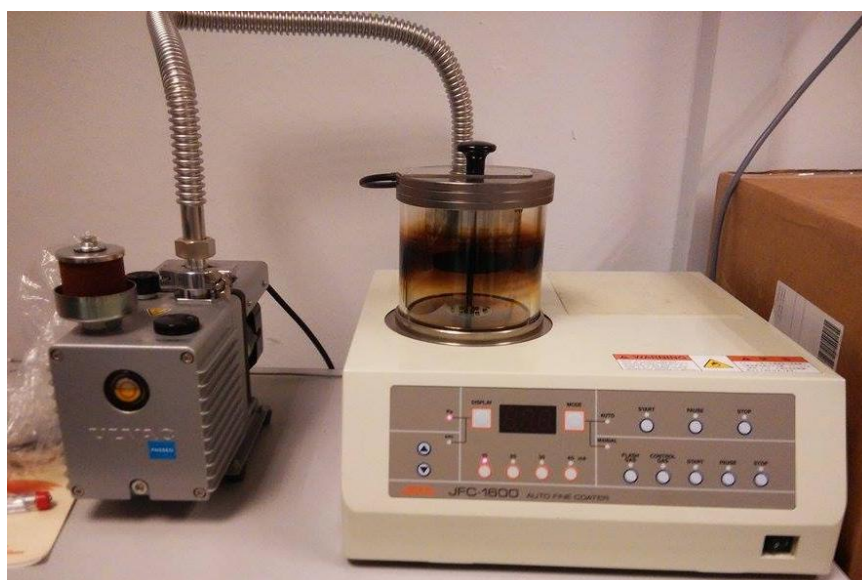


Figure 3.7: JEOL JFC-1600 Auto Fine Coater

3.3.5 Energy-dispersive X-ray Spectroscopy (EDX)

EDX (Octane Silicon Drift Detector by EDAX) is used to analyse the elemental contents on the surface of the catalyst. The analysis was carried out for both alumina pellets and also the prepared catalyst. The applied voltage to do EDX was 20 kV. The figure below shows the FESEM that couples with EDX.



Figure 3.8: JEOL FESEM JSM-6701F

3.3.6 Temperature-programmed Reduction (TPR)

Temperature-programmed reduction (TPDRO 1100 Series by Thermo Scientific) was used to determine the reduction temperature of the catalyst sample. There are two steps involved: pre-treatment and analysis. The purpose of pre-treatment is to remove water and impurities. Table 3.4 below shows the condition employed for both pre-treatment and analysis. Figure 3.7 shows the equipment used for TPR purpose.

Table 3.4: TPR Conditions for Pre-treatment and Analysis

	Pre-treatment	Analysis
Medium/carrier gas	Nitrogen	5.47% hydrogen in nitrogen
Flow rate (mL/min)	25	25
Temperature	110 °C	25 °C to 500 °C
Duration	1 hour	-
Heating ramp	-	5 °C/min



Figure 3.9: TPDRO 1100 Series from Thermo Scientific

CHAPTER 4

RESULTS AND DISCUSSION

4.1 γ -Al₂O₃ Pellet Characterization

Pellet characterization was done prior to determining the support PZC and optimum pH for metal uptake. This is to determine the composition and phase of the pellets. The characterizations carried out here were XRD, SEM and EDX.

4.1.1 XRD Results of γ -Al₂O₃ Pellets

Figure 4.1 shows the analysis results using XRD.

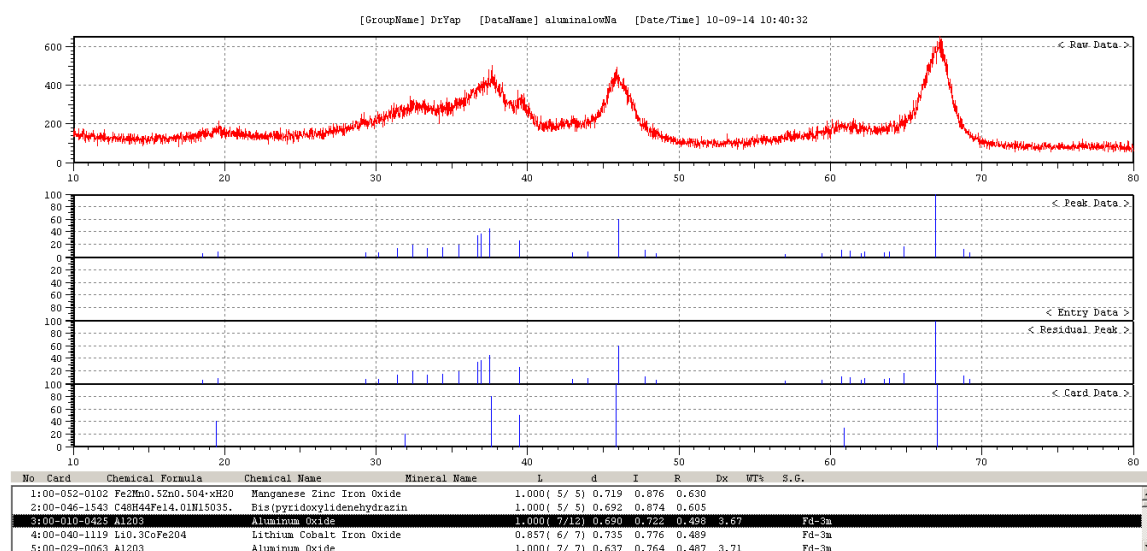


Figure 4.1: XRD Results of γ -Al₂O₃ Pellets

Figure 4.1 shows the X-ray peaks of the γ -Al₂O₃ pellet sample. Sample match was conducted using the library database of XRD (ICDD, International Center Diffraction Data). It shows that aluminium oxide is one of the most possible compounds for the sample tested. Thus it could be concluded that the pellet is made of aluminium oxide. Report generated by XRD could be found in Appendix D.

4.1.2 SEM Image and EDX Results of Alumina Pellets

The figure below shows the SEM image of alumina pellet at 5000 times magnification.

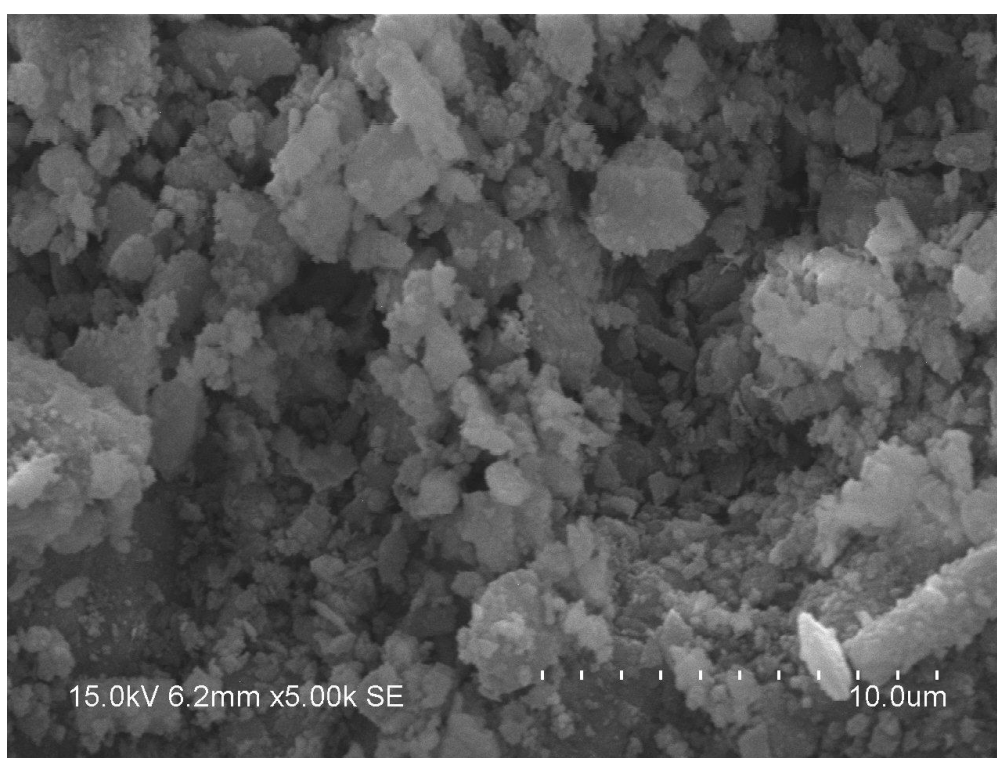


Figure 4.2: SEM Image of γ -Al₂O₃ Pellet with 5000X magnification

From the SEM image, it could be seen that the surface of alumina pellet is porous with a lot of air pockets. The surface is also rough and tortuous. EDX was conducted to determine the elemental composition, and the results could be found in

Appendix E. The results show that the pellets contain magnesium and calcium other than aluminium and oxygen. Thus the alumina pellets contain impurities.

4.2 Support PZC

Before preparing the catalysts, the support PZC was determined. The table below shows the initial pH and the final resulting pH after the addition of $\gamma\text{-Al}_2\text{O}_3$ for different surface loadings. The data presented in Table 4.1 are plotted in Figure 4.3.

Table 4.1: Initial and final pH for different surface loadings

Initial pH	Final pH		
	SL = 50 m ² /L	SL = 500 m ² /L	SL = 1000 m ² /L
1.93	2.14	2.08	2.35
2.51	2.70	2.71	3.15
3.56	3.80	6.32	7.34
4.74	7.40	6.90	7.66
5.71	7.16	7.31	7.82
6.59	7.12	8.42	7.72
7.20	7.53	8.64	8.07
8.92	8.47	8.80	8.65
9.46	9.10	8.72	7.72
10.43	10.33	9.84	8.88
11.10	10.90	10.47	9.84

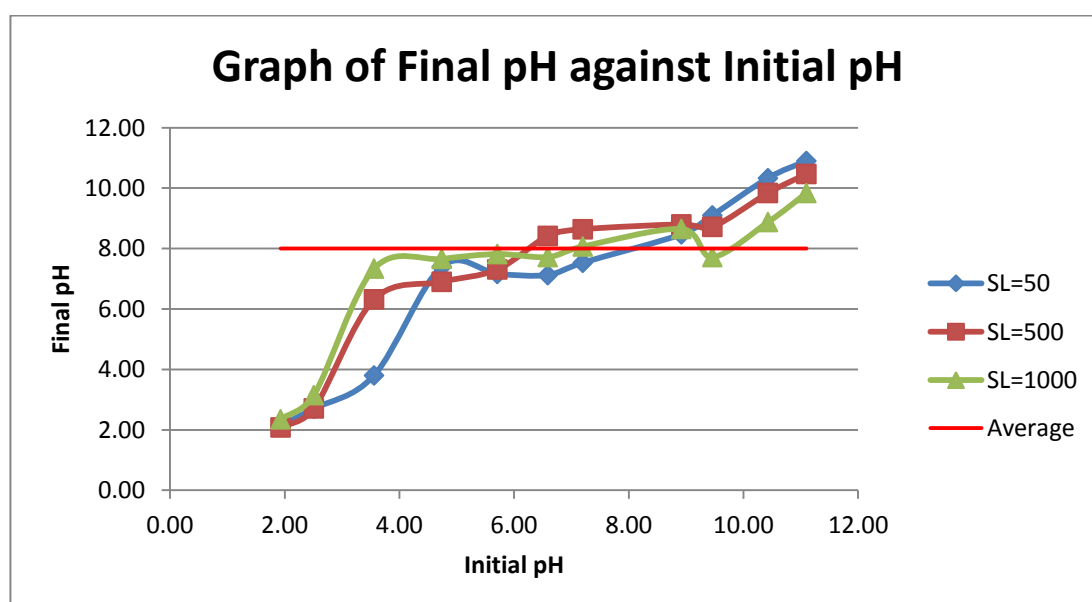


Figure 4.3: Graph of final pH against initial pH for different Surface Loadings

From Figure 4.3 above, it could be seen that there is an approximate plateau appearing at around pH 8. This indicates that final pH at equilibrium is pH 8. Therefore, it could be concluded that PZC for the γ -Al₂O₃ support is approximately at pH 8. At the support PZC, terminal hydroxyl groups are neutral and there is little adsorption of the metal onto the support surface.

One thing to be taken note is that for high surface loading, the rate of change of final pH relative to initial pH is larger. For the same initial pH, the highest surface loading would result in relatively stable final pH. This is due to high amount of OH groups in the support relative to the impregnating solution. Thus it is difficult to charge all the OH groups with little amount of impregnating solution.

4.3 Optimum pH for Metal Uptake

After knowing the support PZC, the optimum pH for metal uptake was determined experimentally to ensure maximum adsorption of platinum particles. Table 4.2 shows the pH, concentration and calculated results for surface density of alumina pellets for different pH. The concentration measured from ICP-OES could be found in Appendix F.

Table 4.2: pH and Surface Density of γ -Al₂O₃ Pellets

pH		Concentration (ppb)		Concentration (mg/L)		Surface density (nmol/m ²)
Initial	Final	Initial	Final	Initial	Final	
1.62	1.62	98.68	82.53	0.09868	0.08253	0.137975
9.03	3.13	227.30	165.10	0.22730	0.16510	0.531395
3.63	3.58	78.61	61.70	0.07861	0.06170	0.144468
3.66	3.96	106.90	71.86	0.10690	0.07186	0.299358
4.99	4.23	65.60	46.78	0.06560	0.04678	0.160785
4.86	5.62	149.80	148.30	0.14980	0.14830	0.012815
7.46	6.35	149.60	124.80	0.14960	0.12480	0.211875
7.66	6.81	141.40	110.30	0.14140	0.11030	0.265698
9.75	8.05	151.80	141.30	0.15180	0.14130	0.089705
10.66	10.88	285.60	281.30	0.28560	0.28130	0.036736

The graph below was plotted based on final pH and surface density.

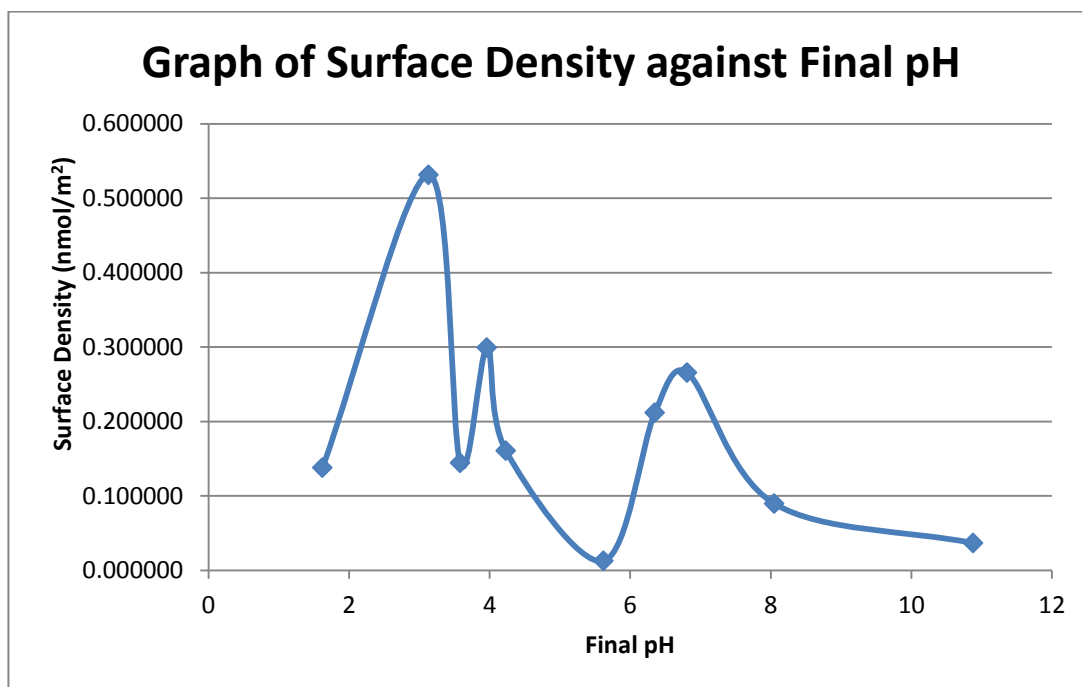


Figure 4.4: Graph of Surface Density against Final pH

This experiment was carried out to investigate the effect of charged surface (via pH) on the degree of metal uptake by γ -Al₂O₃ pellets. As depicted by Figure 4.4, surface density indicates the amount of metal uptake by the γ -Al₂O₃ support. Thus it can be seen that the optimum pH for metal uptake for the γ -Al₂O₃ pellet is at pH 3, which is considerably far from the support PZC. For pH at the extremes (extremely basic or acidic), there were ionic strength inhibition, which causes metals not to be adsorbed onto alumina pellets. Thus there is little metal uptake. At the PZC of support (around pH 8), the surface were not sufficiently charged, and thus resulting in poor metal uptake.

Zhu *et al.* (2013) have also done the simulation on strong electrostatic adsorption at high surface loadings. From their results, the optimum final pH for adsorption is also pH 3. Thus the result obtained from this experiment is satisfactory.

4.4 Egg-shell Profile

4.4.1 Metal Distribution on Alumina

After preparing the catalysts, the cross-section of the pellet is obtained. Figure 4.5 below shows the resulting alumina pellet prepared using dry impregnation (Sample A) after calcination. The white colour part is the cross-section (flat surface) whereas the grey-black colour is the outer surface of the sphere before the pellet is cut.



Figure 4.5: Metal distribution of sample A (the circled part indicates the flat surface)

It could be seen that the surface is grey-black in colour, whereas the center part of the pellet is in white colour. This means that platinum is only adsorbed onto the surface of the alumina pellets and not diffused into the center. This type of metal distribution is known as egg-shell metal distribution.

According to Marceau *et al.* (2009), the egg-shell distribution could be synthesized because there exists a strong interaction between CPA and alumina pellets. The adsorption of CPA onto active sites is strong. When the pellets are subjected to impregnation, CPA quickly finds active sites on the outer surface of the pellet and adsorbed onto it. The hydraulic pressure exerting on the pellet also

reduces as the solution is sucked into the pellet; hence the solution could not diffuse into the pellet center and remains unoccupied.

For the preparation of egg-shell catalyst, the drying temperature employed is to ensure that constant rate period dominates and thus the solution that were transported to the center could be redistributed back to the external surface.

The pH employed to do charge-enhanced dry impregnation method was set to pH 3 since it was determined experimentally (from Figure 4.4) to be the most optimum pH for metal uptake. Figure 4.6 shows the pellet prepared using charge-enhanced dry impregnation (Sample B).



Figure 4.6: Metal distribution of Sample B

From Figure 4.6, it can be seen that the colour on the outer surface of the pellet is not as dark as the catalysts prepared by conventional dry impregnation method. This might be due to the high amount of hydrochloric acid added that have reduced the particle size of platinum to nanoparticles and become more dispersed, and hence it is not visible by naked eye.

From the cross-sectional view of a pellet produced by this method, it could be seen that there is a faint annulus at the surface of the pellet. That annulus is suspected

to be platinum. As verified by TPR results (Section 4.6), there is platinum present on the γ -Al₂O₃ pellet.

4.4.2 FESEM Images and EDX Results

Figure 4.7 shows the FESEM results for sample A synthesized. It is clear from the picture that the surface is porous and rough. The potential platinum particles are highlighted where the size of the nanoparticles is up to nanometers. However, this cannot be confirmed without the use of more sophisticated microscope such as transmission electron microscope (TEM).

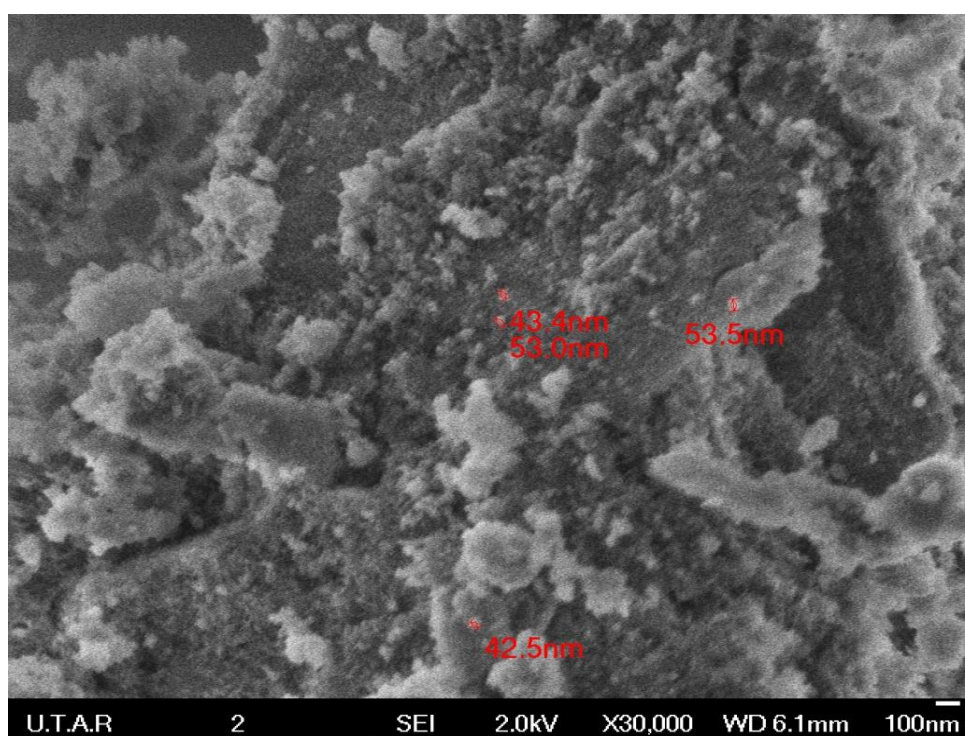
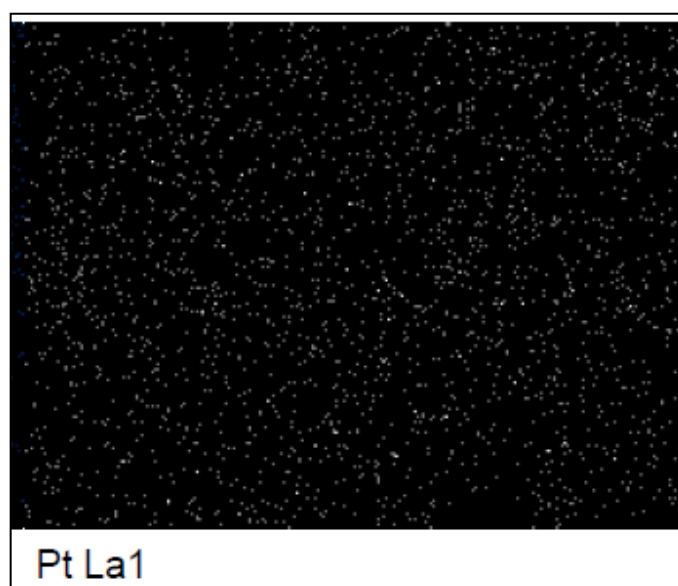


Figure 4.7: FESEM image of Sample A

Figure 4.8 shows the platinum particles mapping using EDX. The white colour signifies the location of platinum. The EDX results for sample A shows that there is 5.46 wt% of platinum on the pellet (found in Appendix F). There is also small amount of chlorine detected. This might be due to the leftover of chlorine compounds from the use of the chloroplatinic acid as the metal precursor. It is

thought that higher calcination temperature and longer calcination time could evaporate and purge the chlorine compounds from the catalyst.



Element	App Conc.	Intensity Corrn.	Weight%	Weight% Sigma	Atomic%
C K	5.07	0.3583	23.48	0.48	34.43
O K	17.04	0.6675	42.35	0.37	46.62
Na K	0.08	0.8155	0.16	0.04	0.13
Mg K	0.36	0.7674	0.77	0.04	0.56
Al K	13.55	0.8608	26.13	0.22	17.06
Cl K	0.36	0.7077	0.84	0.04	0.42
Ca K	0.26	0.9407	0.46	0.03	0.20
Cu K	0.16	0.7937	0.34	0.09	0.09
Pt M	2.23	0.6784	5.46	0.16	0.49

Figure 4.8: Platinum Particles Mapping and Element Percentage of Sample A by EDX

Figure 4.9 shows the FESEM image for sample B. The potential platinum particles are highlighted. Similar to Sample A, it can be seen that the surface is porous and rough. It is also not possible to directly observe the Pt nanoparticles without the use of TEM. Despite that, result from Zhu *et al* (2013) has shown that catalyst with higher metal dispersion could be obtained with charge enhanced dry impregnation method.

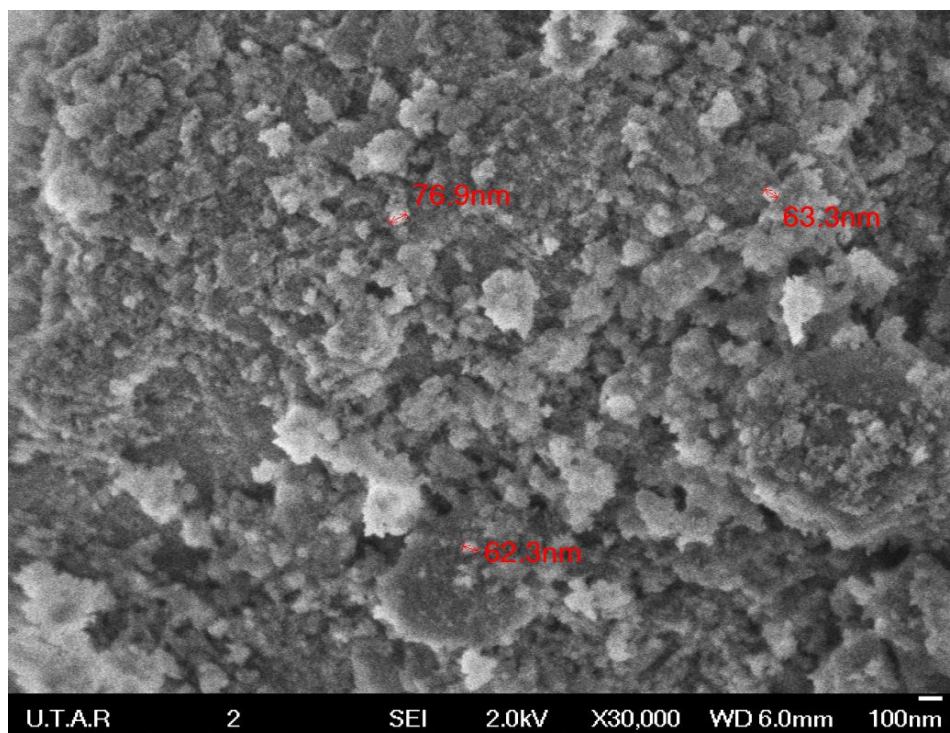


Figure 4.9: FESEM Image of Sample B

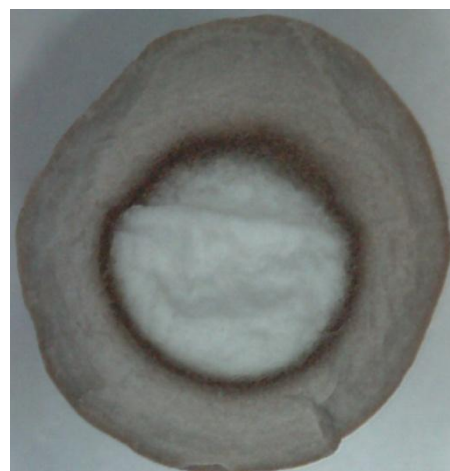
4.5 Egg-white Profile

4.5.1 Metal Distribution on Alumina

Figure 4.10 shows the cross section of egg-white catalysts produced by the conditions as stated in Table 3.3.



(a)



(b)

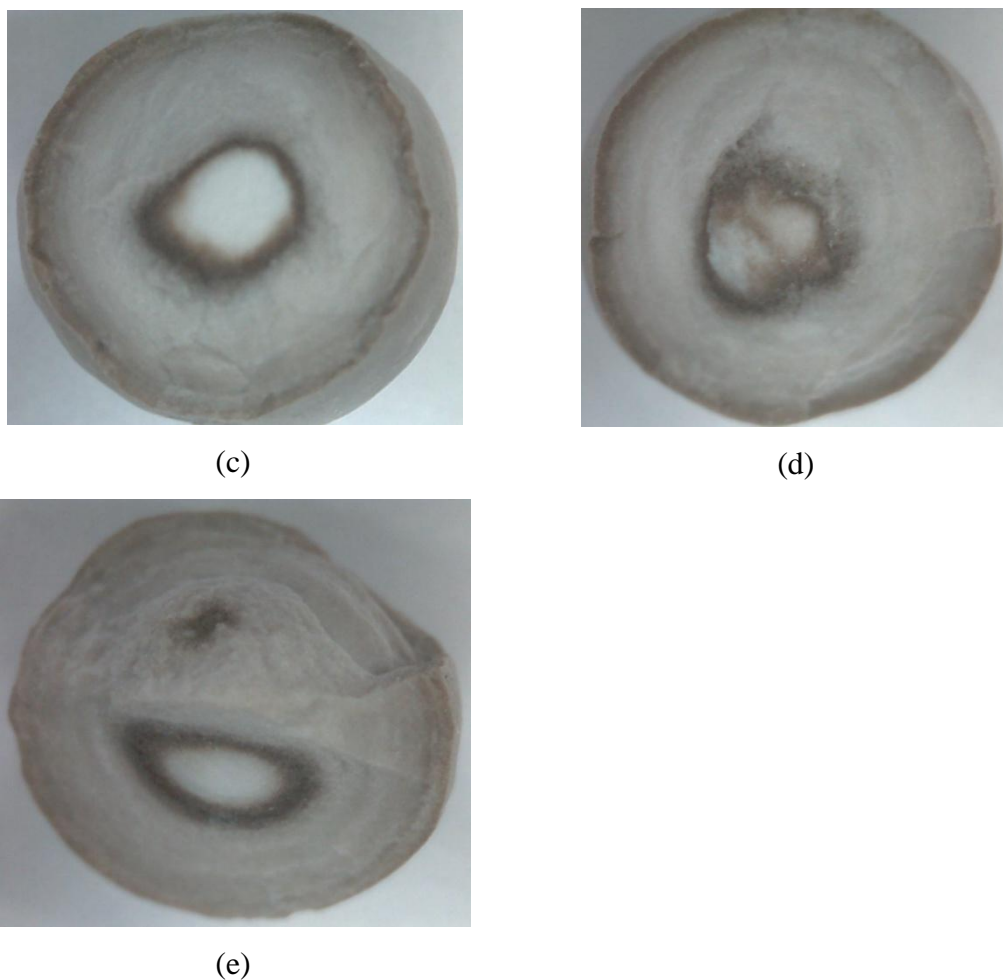


Figure 4.10: Metal Distribution on Alumina; (a) Sample C, (b) Sample D, (c) Sample E, (d) Sample F, and (e) Sample G

From visual inspection on Figure 4.10, the grey-black colour represents the location where platinum nanoparticles are deposited. A darker colour on the picture may indicate a higher density of platinum nanoparticles while location with white colour may represent area with none or low density of platinum nanoparticles.

It can be seen that rings of dark grey colour are located closer to the core of the catalyst from Sample C to Sample G. This corresponds to the use of increasing concentration of citric acid in the impregnating solution. In the preparation of egg-white catalysts, citric acid acts as a coimpregnant, or competitor, that competes with CPA for active sites in alumina pellets. Thus, it could be inferred that citric acid competed with CPA for active sites on the surface. Platinum thus penetrates deeper so that they could adsorb on other active sites.

It is known that the bonding between citric acid and alumina pellet is stronger than the bonding of CPA and alumina (Heise and Schwarz, 1990). For this, wet impregnation is used to prepare egg-white profile catalyst. Since there is an excess of solution used during impregnation, the hydraulic pressure exerting on the pellets is high and this will allow CPA to diffuse deeper into the pellet.

For the same impregnation time with different concentrations of citric acid (samples D, F and G), the platinum ring travels deeper down to the pellet center as the concentration of citric acid increases. As concentration of citric acid increases, more citric acid competes with CPA for active sites. Since adsorption takes place from the pellet surface towards the pellet center, when higher concentration of citric acid is used, more surface layers would be occupied by citric acid. Hence, it could be seen that platinum is only occupied at near the pellet center when concentration of citric acid is high (samples F and G).

Sample E has different impregnation time with sample F using the same molar concentration of citric acid. From the figures above, it could be seen that the position of the platinum ring is almost the same for both cases. Thus it could be inferred that the profile of the catalyst is already established in the first 30 minutes.

Sample C has different impregnation time (15 minutes) and drying conditions (180 °C for 4 hours) as the other samples. Since the drying is fast at 180 °C, and the concentration of citric acid is low, the platinum ring is located relatively near to the pellet surface. At 180 °C, partial calcination has taken place as when the pellets were taken out from the oven; some of them appeared to be grey in colour.

Egg-yolk catalyst profile was not able to prepare in this project due to the nature of the support pellet. The alumina pellets were found to be made from two distinctive layers between the outer layer and the inner core, and thus making it difficult for the CPA to diffuse into the core of the pellet.

4.5.2 FESEM Image and EDX Result

Figure 4.11 shows the FESEM image of sample C. The magnification is 70 000X where it could measure up to the scale of nanometers. The potential platinum particles are highlighted in the image.

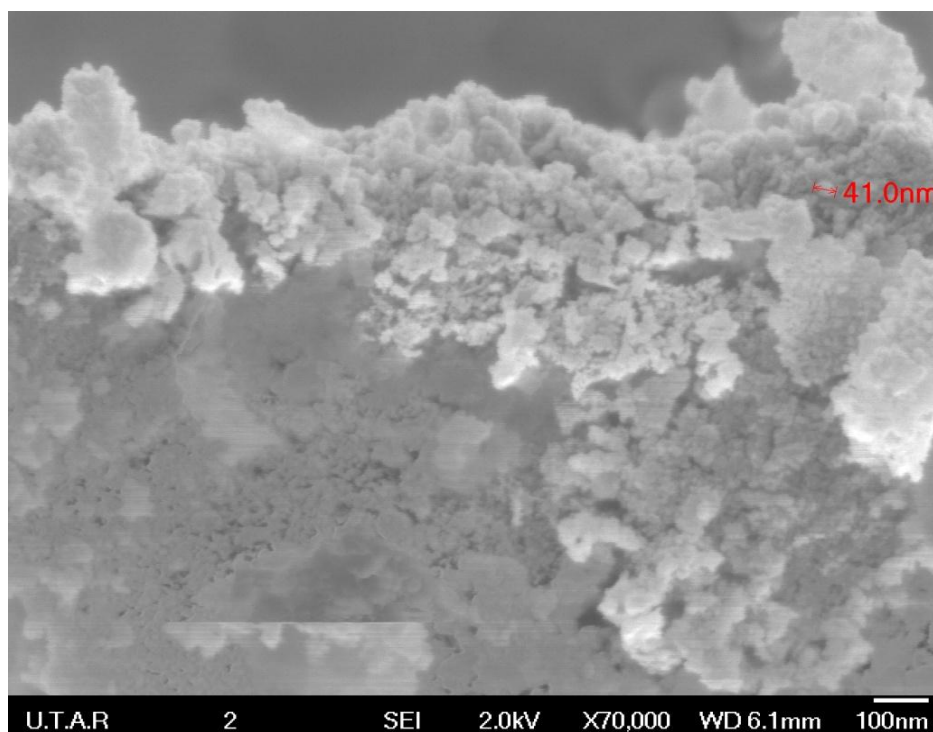
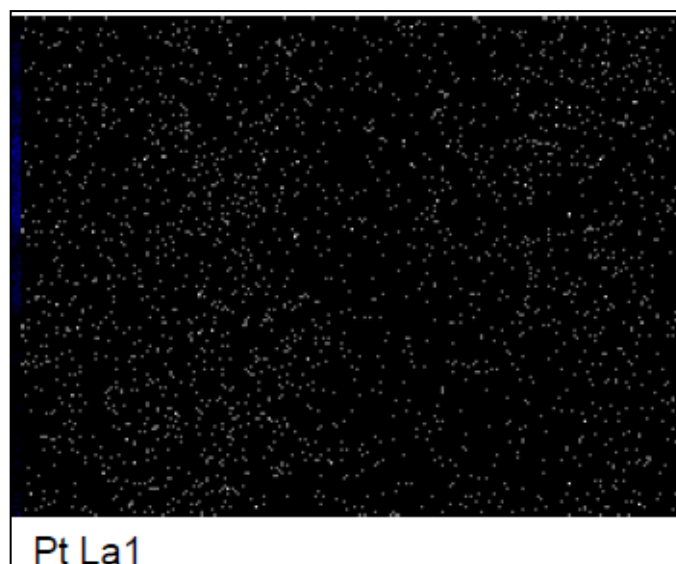


Figure 4.11: FESEM Image of Sample C

Figure 4.12 shows the platinum particles mapping of sample C by EDX. The mapping shows that the density of platinum is not as high as in sample A. The EDX result of the sample shows that there is 0.63 wt% of platinum on the pellet. The lower level of platinum indicates that the sample might not be positioned to face the detector. Similar to the EDX result obtained for egg-shell catalysts, there is also chlorine detected due to incomplete decomposition of chlorine. The complete report and the mapping could be found in Appendix G. Copper and zinc were also detected in EDX which might be due to contamination.



Element	App Conc.	Intensity Corrn.	Weight%	Weight% Sigma	Atomic%
C K	0.86	0.2973	17.24	0.57	25.75
O K	5.69	0.7640	44.81	0.41	50.23
Al K	4.99	0.8588	34.82	0.31	23.15
Cl K	0.06	0.7002	0.55	0.04	0.28
Cu K	0.14	0.7905	1.02	0.15	0.29
Zn K	0.12	0.7876	0.92	0.18	0.25
Pt M	0.07	0.6214	0.63	0.12	0.06

Figure 4.12: Platinum Particles Mapping and Element Percentage of Sample C using EDX

4.6 TPR Results

TPR is used to determine the reduction temperature of the catalysts prepared, and thereby deduce the compounds present. In a TPR to characterize the catalyst, hydrogen is adsorbed onto the active sites of alumina and for the reduction of platinum oxide.

Figure 4.13 shows the superimposed curves obtained for different samples. From the report generated by TPDRO (found in Appendix H) for sample A (eggshell DI), sample B (egg-shell CEDI) and sample C (egg-white CA 0.2), the peaks appear at around 212 °C.

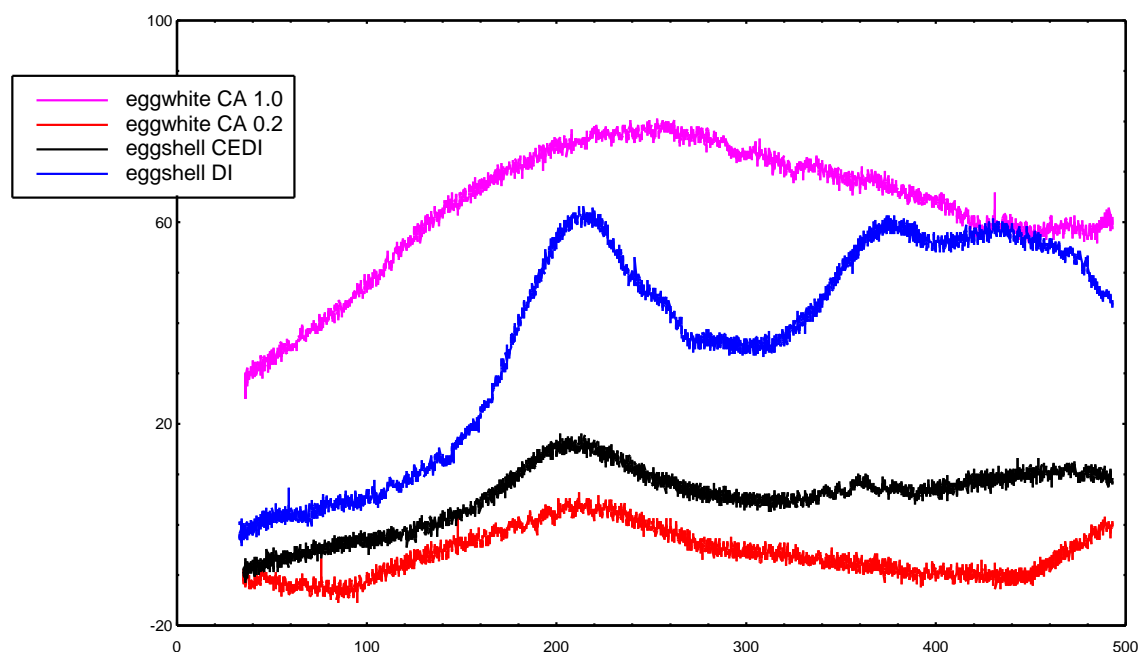


Figure 4.13: TPR Curves for Sample A (egg-shell DI), Sample B (egg-shell CEDI), Sample C (egg-white CA 0.2) and Sample E (egg-white CA 1.0)

The peaks appeared suggests that the optimum reduction temperature of the prepared catalyst is at 212 °C. Similar observation was also obtained by Cho (2013) where the peak appeared at 210 °C. On the other hand, Sample E (egg-white CA 1.0) appears to have a different peak at 249 °C.

An interesting trend can be seen where both sample C and sample E have a single peak at 210 – 240 °C, while there are two peaks appear for both sample A and sample B where a peak is located at around 212 °C and another peak is located at 360 – 380 °C. Both sample C and sample E are prepared by wet impregnation method while sample A and sample B are prepared *via* dry impregnation method.

According to Lieske *et al.* (1983) and Hwang and Yeh (1996), the peak at 212 °C can be attributed to PtAl_2O_4 species (reduction temperature at 220 °C, difference in temperature might be due to difference in metal loading), while the peak observed at 380°C – 400°C are thought to be Pt oxychlorinated species. Comparing EDX results of sample A and sample C, it could be seen that the chlorine composition in sample A is higher (0.84 wt%) compared to that of sample C (0.55 wt%), which might have caused the discrepancy in TPR peaks. Dry impregnation to

produce egg-shell catalysts which employs higher concentration of CPA (0.24 M) than wet impregnation (0.04 M) would result in higher content of chlorine. Therefore, the leftover chlorine that has combined with oxygen on the support surface was reduced at a temperature between 380°C – 400°C.

The area under the curves signifies the amount of adsorbed hydrogen. From the report and curves generated, it could be seen that sample A has 366.14474 $\mu\text{mol/g}$ of hydrogen adsorbed, which is high compared to sample B (168.76492 $\mu\text{mol/g}$) and sample C (103.38735 $\mu\text{mol/g}$). This is due to the high amount of platinum adsorbed and hence more hydrogen is required to reduce the platinum.

For sample E, since the curve generated shows that the peak is relatively broad; when analyzed it results in a higher reduction temperature, and also highest amount of hydrogen adsorbed compared to the other samples. The results might not be conclusive as there might be interference present.

CHAPTER 5

CONCLUSION AND RECOMMENDATIONS

5.1 Conclusion

In this project, Pt/ γ -Al₂O₃ catalysts with non-uniform distribution of platinum particles have been prepared and characterized.

The project objectives have been achieved where:

- Pt/ γ -Al₂O₃ catalysts with egg-shell profile have been prepared using conventional dry impregnation (DI), and charge enhanced dry impregnation (CEDI)
- Pt/ γ -Al₂O₃ catalysts with egg-white profile have been prepared using wet impregnation method
- high concentration of precursor solution could be used to prepare egg-shell catalysts whereas low concentration of precursor solution with co-impregnants could be used to prepare egg-white catalysts
- drying conditions did not affect the metal distribution drastically

Egg-shell catalysts could be prepared by both dry impregnation and charge-enhanced dry impregnation method. To prepare egg-shell catalysts:

- a) Solution should have high concentration of platinum.
- b) Drying rate is slow so that metals in the pellet center could be redistributed back to the surface.
- c) Hydrochloric acid added could reduce the size of platinum particles.

For egg-white catalysts, wet impregnation method is used so that the hydraulic pressure exerted on the pellet could push the solution towards the pellet center. To prepare egg-white catalysts:

- a) Competitor is added; in this project the competitor added is citric acid.
- b) Concentration of platinum should be low.
- c) Drying whether at high temperature or relatively low temperature did not affect the metal profile drastically. However, drying at 180 °C causes partial calcination to occur.

Egg-yolk catalysts are relatively difficult to synthesize due to the nature of the support pellet. It might be difficult for the solution to diffuse into the pellet center.

5.2 Recommendations

While this report covers many important grounds on the preparation and characterization of Pt/ γ -Al₂O₃ catalyst with non-uniform distribution, there are significant gaps that have to be filled in order to paint a better overall picture. Hence, the following recommendations are suggested to future researchers who will work on this topic:

- a) There is a need to replace the γ -Al₂O₃ pellet used in this project where the pellets possess two distinctive layers that prevent the impregnating solution from diffusing towards the core of the pellet. The new type of pellets should have a more consistent overall structure.
- b) When above issue can be resolved, egg-yolk profile catalyst can be prepared and this will allow comparison with the egg-shell and egg-white catalysts that have been prepared in this project
- c) Transmission electron microscopy (TEM) characterization should be carried out to study the size and dispersion of metal nanoparticles.
- d) Hydrogen chemisorption study can be performed to obtain the dispersion of metal catalyst, and this can be used to verify the TEM of the nanoparticles.
- e) Nitrogen adsorption study on the alumina pellets should be carried out to determine the BET surface area and pore volume of the pellets.

REFERENCES

- Arsalanfar, M., Mirzaei, A.A., Bozorgzadeh, H.R., Samimi, A., and Ghobadi, R., 2013. Effect of support and promoter on the catalytic performance and structural properties of the Fe-Co-Mn catalysts for Fischer-Tropsch synthesis. *Journal of Industrial and Engineering Chemistry*, 20(2014), pp. 1313- 1323.
- Bagheri, S., Muhd Julkapli, N., and Abd Hamid, S., 2014. Titanium dioxide as a catalyst support in heterogeneous catalysis. *The Scientific World Journal*, 2014(2014), 21 pages.
- Campanati, M., Fornasari, G., and Vaccari, A., 2003. Fundamentals in the preparation of heterogeneous catalysts. *Catalysis Today*, 77(2003), pp. 299-314.
- Cao, C., Yang, G., Dubau, L., Maillard, F., Lambert, S.D., Pirard, J., and Job, N., 2014. Highly dispersed Pt/C catalysts prepared by the charge enhanced dry impregnation method. *Applied Catalysis B: Environmental*, 150-151(2014), pp. 101-105.
- Cho, H.R., 2013. *The rational synthesis of supported noble single or bimetallic catalysts by electrostatic adsorption*. PhD. University of South Carolina.
- Clark, J., 2013. *Types of catalysis*. [online] Available at <<http://www.chemguide.co.uk/physical/catalysis/introduction.html>> [Accessed 18 June 2014]
- De Jong, K.P., 2009. *Synthesis of solid catalysts*. Germany: Wiley-VCH.
- Farias, F.E.M., Neto, R.C.R., Baldanza, M.A.S., Schmal, M., and Fernandes, F.A.N., 2011. Effect of K promoter on the structure and catalytic behaviour of supported iron-based catalysts in Fischer-Tropsch synthesis. *Brazilian Journal of Chemical Engineering*, 28(3).
- Gao, M., Lyalin, A., and Taketsugu, T., 2011. Role of the support effects on the catalytic activity of gold clusters: A density functional theory study. *Catalysis*, 1, pp. 18-39.
- Grecian Magnesite, n.d. *Catalysts*. [online] Available at: <<http://www.grecianmagnesite.com/markets/industrial-chemical/catalysts>> [Accessed 4 April 2015]

- Haber, J., Block, J.H., and Delmon, B., 1995., IUPAC: Manual of methods and procedure catalyst characterization. *Pure & Applied Chemistry*, 67(8), pp. 1257-1306.
- Hager, G.T., Ochoa, R., Givens, E.N., Eklund, P.C., and Derbyshire, F.J., n.d. *The effect of promoter metals on the catalytic activity of sulphated hematite for model compound reactions*. University of Kentucky.
- Heise, M.S., and Schwarz, J.A., 1985. Preparation of metal distributions within catalyst supports – Effect of pH on catalytic metal profiles. *Journal of Colloid and Interface Science*, 153(1).
- Heise, M.S., and Schwarz, J.A., 1986. Preparation of metal distributions within catalyst supports – Effect of ionic strength on catalytic metal profiles. *Journal of Colloid and Interface Science*, 113(1).
- Heise, M.S., and Schwarz, J.A., 1988. Preparation of metal distributions within catalyst supports – Single component modelling of pH, ionic strength and concentration effects. *Journal of Colloid and Interface Science*, 123(1).
- Heise, M.S., and Schwarz, J.A., 1990. Preparation of metal distributions within catalyst supports – Multicomponent effects. *Journal of Colloid and Interface Science*, 135(2).
- Hodar, F.J.M., 2009. *Heterogeneous catalysis (I)*. [online] Available at: <<http://www.unicam.it/discichi/acaoc/lectures/Maldonado%201.pdf>> [Accessed 20 February 2015]
- Hwang, C.P., and Yeh, C.T., 1996. Platinum-oxide species formed by oxidation of platinum crystallites supported on alumina. *Journal of Molecular Catalysis A: Chemical*, 112(2), pp. 295-302.
- Kim, B.G. *et al.*, 2014. Improved reversibility in lithium-oxygen battery: Understanding elementary reactions and surface charge engineering of metal alloy catalyst. *Scientific Reports* 4. [online] Available at <<http://www.nature.com/srep/2014/140227/srep04225/full/srep04225.html>> [Accessed 17 February 2015]
- Laosiripojana, N., and Assabumrungrat, S., 2006. The effect of specific surface area on the activity of nano-scale ceria catalysts for methanol decomposition with and without steam at SOFC operating temperatures. *Chemical Engineering Science*, 61(2006), pp. 2540-2549.
- Lieske, H., Lietz, G., Spindler, H., and Volter, J., 1983. Reaction of platinum in oxygen and hydrogen treated Pt/h-Al₂O₃ catalysts. *Journal of Catalysis*, 81, pp. 8-14.

- Lin, C., Tao, K., Hua, D., Ma, Z., and Zhou, S., 2013. Size effect of gold nanoparticles in catalytic reduction of p-nitrophenol with NaBH₄. *Molecule*, 18, pp. 12609-12620.
- Liu, W., and Roy, S., 2004. Effect of channel shape on gas/liquid catalytic reaction performance in structured catalyst/reactor. *Chemical Engineering Science*, 59(2004), pp. 4927-4939.
- Mohammed, A.A.K., Gaib, M., and Abbass, M.N., 2008. Effect of promoters on the catalytic activity of the isomerisation catalyst. *Iraqi Journal of Chemical and Petroleum Engineering*, 9(1), pp. 9-14.
- Mohanty, P., Pant, K.K., Naik, S.N., Parikh, J., Hornung, A., and Sahu, J.N., 2014. Synthesis of green fuels from biogenic waste through thermochemical route – The role of heterogeneous catalyst: A review. *Renewable and Sustainable Energy Reviews*, 38(2014), pp. 131-153.
- Morbidelli, M., Gavriilidis, A., and Varma, A., 2001. *Catalyst design: Optimal distribution of catalyst in pellets, reactors and membranes*. Cambridge: Cambridge University Press.
- Moss, R.L., 1967. The structure of supported platinum catalysts: Examination by electron microscopy. *Platinum Metals Rev.*, 11(4), pp. 141-145.
- Papageorgiou, P., Price, D.M., Gavriilidis, A., Varma, A., 1995. Preparation of Pt/ γ -Al₂O₃ pellets with internal step-distribution of catalyst: Experiments and theory. *Journal of Catalysis*, 158, pp. 439-451.
- Park, D., Kim, S.M., Kim, S.H., Yun, J.Y., and Park, J.Y., 2014. Support effect on the catalytic activity of two-dimensional Pt nanoparticle arrays on oxide substrates. *Applied Catalysis A: General*, 480(2014), pp. 25-33.
- Ralphs, K., Hardacre, C., James, S.L., 2013. *Application of heterogeneous catalysts prepared by mechanochemical synthesis*. [online] Available at: <<http://pubs.rsc.org/en/Content/ArticleLanding/2013/CS/c3cs60066a#!divAbstract>> [Accessed 22 June 2014]
- Regalbuto, J.R., 2007. *Catalyst preparation science and engineering*. New York: CRC Press.
- Ryberg, S., 2010. Characterization of Pt/CeO₂ catalysts: Thermal aging studies of high surface area support and evaluation of chemisorptions based dispersion measurements. [online] Available at <<http://publications.lib.chalmers.se/records/fulltext/126762.pdf>> [Accessed 20 August 2014]

- School Work Helper, n.d. *Factors that affect rates of reaction*. [online] Available at: <<http://schoolworkhelper.net/factors-that-affect-rates-of-reaction/>> [Accessed 18 February 2015]
- Science HQ, 2013. *Types of catalysts*. [online] Available at: <<http://www.sciencehq.com/chemistry/types-of-catalysts.html>> [Accessed 18 June 2014]
- Sharma, R.K., Sharma, P., and Maitra, A., 2003. *Size-dependent catalytic behaviour of platinum nanoparticles on the hexacyanoferrate (III) thiosulfate redox reaction – Abstract*. [online] Available at <<http://www.ncbi.nlm.nih.gov/pubmed/12927175>> [Accessed 25 June 2014]
- Song, C., Hanaoka, K., and Nomura, M., 1991. *Effects of pore structure and support type of catalysts in hydroprocessing of heavy coal liquids*.
- Stephan, D., 2013. *Global catalyst demand to reach US\$19.5 billion in 2016*. [online] Available at: <http://www.process-worldwide.com/management/markets_industries/articles/395298/> [Accessed 18 June 2014]
- Su, F., Lee, F.Y., Lv, L., Liu, J., Tian, X.N., and Zhao, X.S., 2007. Sandwiched ruthenium/carbon nanostructures for highly active heterogeneous hydrogenation. *Advanced Functional Materials*, 17(12), pp. 1926-1931. doi: 10.1002/adfm.200700067.
- The Columbia Electronic Encyclopaedia, 2012. *Types and importance of catalysts*. 6th ed. [online] Available at: <<http://www.infoplease.com/encyclopedia/science/catalyst-types-importance-catalysts.html>> [Accessed 18 June 2014]
- The University of York, 2013. *Catalysis in industry*. [online] Available at: <<http://www.essentialchemicalindustry.org/processes/catalysis-in-industry.html>> [Accessed 22 June 2014]
- Wan Abu Bakar, W.A., Ali, R., and Mohammad, N.S., 2013. The effect of noble metals on catalytic methanation reaction over supported Mn/Ni oxide based catalysts. *Arabian Journal of Chemistry* (2013).
- Wang, Y., Yan, R., Zhang, J., and Zhang, W., 2009. Synthesis of efficient and reusable catalyst for size-controlled Au nanoparticles within a porous, chelating and intelligent hydrogel for aerobic alcohol oxidation. *Journal of Molecular Catalysis A: Chemical*, 317(2010), pp. 81-88.
- Zhu, X., Cho, H., Pasupong, M., and Regalbuto, J.R., 2013. Charge-enhanced dry impregnation: A simple way to improve the preparation of supported metal catalysts, *ACS Catalysis*, 3(2013), pp. 625-630.